

Infinite-ranged models of spin-glasses

Scott Kirkpatrick

IBM Thomas J. Watson Research Center, Yorktown Heights, New York 10598

David Sherrington

IBM Thomas J. Watson Research Center, Yorktown Heights, New York 10598

Physics Department, Imperial College, London, England SW7 2BZ,*

and Institut Louis-Langevin, BP 156, 68092 Strasbourg Cedex, France,*

(Received 5 December 1977)

A class of infinite-ranged random-model Hamiltonians is defined as a limiting case in which the appropriate form of mean-field theory (order parameters and phase diagram) to describe spin-glasses may be established. It is believed that these Hamiltonians may be exactly soluble, although a complete solution is not yet available. Thermodynamic properties of the model, for Ising and XY spins are evaluated using a "many-replica" procedure. Results of the replica theory reproduce properties at and above the ordering temperature which are also predicted by high-temperature expansions, but are in error at low temperatures. Extensive computer simulations of infinite-ranged Ising spin-glasses are presented. They confirm the general details of the predicted phase diagram. The errors in the replica solution are found to be small, and confined to low temperatures. For this model, the extended mean-field theory of Thouless, Anderson, and Palmer gives physically sensible low-temperature predictions. These are in quantitative agreement with the Monte Carlo studies. The dynamics of the infinite-ranged Ising spin-glass are studied in a linearized mean-field theory. Critical slowing down is predicted and found, with correlations decaying as $t^{-1/2}$ for t greater than T_c , the spin-glass transition temperature. At and below T_c , spin-spin correlations are observed to decay to their long-time limit as $t^{-1/2}$.

1. INTRODUCTION

In recent years considerable interest has arisen in the possibility of the existence in suitably disordered systems of a new type of magnetic order not found in pure systems. This is the so-called spin-glass phase^{1,2} in which magnetic moments are believed to be frozen into thermal equilibrium orientations but with no average long-range order; one way of defining this statement mathematically is to say that $\langle \vec{S}_i \vec{S}_j \rangle \neq 0$ but $\langle \vec{S}_i \rangle = \langle \vec{S}_j \rangle = 0$ as $\vec{R}_i = \vec{R}_j = 0$, where $\langle \dots \rangle$ refers to a thermal average and $\langle \dots \rangle_s$ to an average over the spatial disorder (in the latter case with $\vec{R}_i = \vec{R}_j$ held fixed).

A number of physical examples appear to exist; the canonical cases³ are metallic alloys with substitutional magnetic impurities, such as CuMn or FeFe; other examples are found in amorphous systems and in compounds with inequivalent sites randomly available to magnetic ions. A necessary requirement seems to be a locally random competition between ferromagnetic and antiferromagnetic forces, although this competition may have a number of possible microscopic origins: for example, fixed positions but random exchange, fixed exchange interaction as a function of distance but random positions, topological disorder as in an amorphous system with antiferromagnetic exchange but no possibility of a valdation, etc.

In order to demonstrate theoretically the pos-

sible existence of a spin-glass phase Edwards⁴ and Anderson⁵ (EA) introduced a simple model with exchange disorder and were able within a novel mean-field theory to demonstrate the existence of the phase. Their model is of a set of classical spins \vec{S}_i on a periodic lattice interacting via an exchange interaction

$$H = - \sum_{ij} J_{ij} \vec{S}_i \cdot \vec{S}_j, \quad (1.1)$$

where the sum is over nearest-neighbor pairs and the J_{ij} are independently distributed with the Gaussian probability distribution

$$p(J_{ij}) = (2\pi J^2)^{-1/2} \exp(-J_{ij}^2/2J^2). \quad (1.2)$$

The disorder is quenched; that is, J_{ij} 's are chosen randomly but then fixed for all thermodynamic purposes. It is evident that none of the conventional types of order is possible. To study this problem, EA employed a novel replication procedure with spin orientation between Gibbs-like replicas playing the role of a spin-glass order parameter in a generalized mean-field solution. Since that work, extensions have been made⁶ to include interactions beyond nearest neighbors,^{6,7} exchange distributions offset from zero to allow for competition between spin-glass and ferro (or antiferro-) magnetism,⁷ and some quantum effects.⁸⁻¹⁰ These studies have all employed mean-field theories with the unconventional EA order parameter,

It is well known that molecular-field theory for a pure ferromagnet becomes exact in the thermodynamic limit for a constant infinite-range exchange interaction provided that the interaction is appropriately scaled with the number of spins in the system.⁷ In this paper, we examine the analogous situation for systems which can exhibit spin-glass and ferromagnetic behavior. The Hamiltonians we employ are analogous to (1.1) but the summation $\sum_{i,j}$ runs over all pairs of sites (i, j) in the system and we concentrate primarily, but not exclusively, on an Ising interaction. We show that to lead to physical but non-trivial thermodynamic consequences a constant moment of J_{ij} (denoted J_{00}^2) must scale inversely as the number of spins N . Thus, for possible ferromagnetism we require

$$(J_{ij})_c = \bar{J}_0 N^2 + O(N^2) \quad (p > 1), \quad (1.3a)$$

and for potential spin-glass behavior

$$(J_{ij}^2)_{0c} = \bar{J}^2 N^4 + O(N^4) \quad (r > 1). \quad (1.3b)$$

The relative magnitudes of \bar{J}_0 and \bar{J} determine whether ferromagnetism or spin-glass ordering occurs at low temperature. Higher constants will scale as higher inverse powers of N than the first two and thus do not affect the thermodynamic properties of an infinite-ranged model. We shall therefore employ a Gaussian distribution of interactions without loss of generality.

The plan of the paper is as follows. In Sec. II we employ the replication procedure⁸ of EA to analyze an infinite-ranged Ising spin-glass-ferromagnet model with a Gaussian distribution of interactions the moments of which are as given in (1.3a) and (1.3b). A condensed version of Sec. II was originally presented in Ref. 5. In Sec. III, we present a high-temperature series expansion for the same model, which confirms the predictions of the replication procedure for the transition from paramagnet to spin-glass or ferromagnet with decreasing temperature. [This expansion has been described by Thouless *et al.*⁹ (TA)] for the case of pure spin-glass ordering.] In Sec. IV, we investigate the corresponding classical planar spin model using the replication method. As stated earlier we believe the general classical n -vector model based on an infinite-ranged version of (1.1) with distributions scaled as in (1.3) is in principle exactly solvable. Section V reports Monte Carlo tests of the replica and other theories, necessary since no real systems with the assumed approximations are known. The simulations also give access and insight into some of the microscopic phenomena which are unique to spin glasses. Dynamics of spin glasses (assuming Ising interactions and

single spin-flip relaxation processes) are analyzed and then studied by Monte Carlo in Sec. V.

II. REPLICATION THEORY

For purposes of calculation, it is usually convenient to average over any randomness in a physical system at the earliest possible stage. When the randomness is quenched (immobile) the averaging must however be carried out on a physical observable. In the present thermodynamic problem, we must therefore average the free energy F and not, for example, the partition function Z . Normally, this is a much more awkward procedure than that of averaging Z , as would be appropriate to a system with annealed disorder. However, at the cost of increasing the effective spin dimensionality and using limiting procedures, a free-energy average can be transformed into a partition function average using a procedure which appears to have been first used in statistical mechanics by Kac³ but rediscovered independently by Edwards,^{4,10} Grinstein and Luther,¹¹ and Emery.¹² This procedure is essentially the identity

$$\lim_{n \rightarrow 0} \ln (n^2 - 1)/n, \quad (2.1)$$

with n taken as the partition function Z . For integral n , Z^n may be expressed as

$$Z^n = \int \prod_{\alpha=1}^n Z_{\alpha}, \quad (2.2)$$

where α is a dummy label. The set $\alpha = 1, \dots, n$ may be interpreted as identical replicas of the real system. In a disordered system Z_{α} is a function of the disorder, all the replicas α having the same disorder but not interacting in any way with one another. Averaging the free energy over the disorder leads, via (2.1), to an averaging of Z^n over the disorder. For the case of integral n , averaging Z^n leads in turn to an effective interaction between the replicas α and thus to an effective pure system with an interaction of higher order than the real (impure) system. This effective system is analytically continued to small n to give the averaged free energy using (2.1). In this section, we apply this replica procedure to the infinite-ranged Ising model with Gaussian exchange distribution.

The system we consider here is characterized by the Hamiltonian

$$\mathcal{H} = - \sum_{i,j} J_{ij} S_i S_j - H \sum_i S_i, \quad (2.3)$$

where the spin operators S_i take the values ± 1 , the (i,j) sum is over all bonds, the J_{ij} are dis-

distributed according to

$$p(\{J_{ij}\}) = (12\pi)^{1/2} j^{-1} \exp \frac{-\{J_{ij}\}^2 - j^2}{2j^2}, \quad (2.4)$$

and H is an external field. Using (2.1) and (2.2) the averaged free energy per spin, $f(-J/\lambda)$ in the thermodynamic limit may be expressed as

$$f = -kT \lim_{N \rightarrow \infty} \lim_{n \rightarrow 0} (nN)^{-1} \left\{ \int \prod_{i,j} [p(\{J_{ij}\}) dJ_{ij}] \text{Tr}_n \exp \left[\sum_{\alpha, \beta} \left(\sum_{i,j} J_{ij} S_i^\alpha S_j^\beta / kT + H \sum_i S_i^\alpha / kT \right) \right] - 1 \right\} \quad (2.5)$$

$$= -kT \lim_{N \rightarrow \infty} \lim_{n \rightarrow 0} (nN)^{-1} \left\{ \text{Tr}_n \exp \left[\sum_{i,j} \left(\sum_{\alpha} S_i^\alpha S_j^\alpha J_{\alpha} / kT + \sum_{\alpha, \beta} S_i^\alpha S_j^\beta S_i^\beta S_j^\alpha / 2(kT)^2 \right) + \frac{H}{kT} \sum_i \sum_{\alpha} S_i^\alpha \right] - 1 \right\}, \quad (2.6)$$

where α, β label n dummy replicas and Tr_n denotes the trace over spins in each of the n replicas. After some rearranging we obtain

$$f = -kT \lim_{N \rightarrow \infty} \lim_{n \rightarrow 0} (nN)^{-1} \left[\exp \left\{ -\frac{1}{2} (J^2 - 4(kT)^2)(\lambda^2 n - n^2 N) - (H^2 / 2kT)(\lambda n) \right\} \text{Tr}_n \exp \left(\frac{J^2}{2kT} \sum_{\alpha} \left(\sum_i S_i^\alpha \right)^2 \right. \right. \\ \left. \left. - \frac{J^2}{2(kT)^2} \sum_{\alpha, \beta} \left(\sum_i S_i^\alpha S_i^\beta \right)^2 + \frac{H}{kT} \sum_{\alpha} \sum_i S_i^\alpha \right) - 1 \right], \quad (2.7)$$

where (α, β) refers to combinations of α and β with $\alpha \neq \beta$. Note that the exchange terms in the second exponent are now in the form $\lambda (\sum_i O_i)^2$ where O_i is a local operator, which leads to physical but nontrivial thermodynamic consequences only if $\lambda \sim N^{-1}$. The physically sensible scaling of $J_{\alpha\beta} \sim J$ is, thus,

$$J_{\alpha\beta} = \tilde{J}_{\alpha\beta} / N, \quad (2.8a)$$

$$J = \tilde{J} / N^{1/2}, \quad (2.8b)$$

with $\tilde{J}_{\alpha\beta} \sim \tilde{J}$ both intensive. More complicated dis-

tributions than (2.4) will, in general, give rise to terms of sixth and higher order in (2.8), but these will be of order N^{-1} or smaller, and thus are without thermodynamic consequences.

It also follows from the form $\lambda (\sum_i O_i)^2$ that a transformation may be made to a Gaussian-averaged single-site problem, using the identity

$$\exp(\lambda n^2) = (2\pi)^{-1/2} \int dx \exp \left[-\frac{1}{2} x^2 + (2\lambda)^{1/2} nx \right], \quad (2.9)$$

Dropping terms which vanish in the thermodynamic limit, we may rewrite (2.7) as

$$f = -kT \lim_{N \rightarrow \infty} \lim_{n \rightarrow 0} (nN)^{-1} \left(\exp[\tilde{J}^2 N n / 4(kT)^2] \int \left[\prod_{\alpha} \left(\frac{N}{2\pi} \right)^{1/2} d\alpha^{\alpha} \right] \left[\prod_{\alpha, \beta} \left(\frac{N}{2\pi} \right)^{1/2} d\alpha^{\alpha\beta} \right] \right. \\ \left. \times \exp \left\{ -N \left[\sum_{\alpha} \frac{1}{2} (x^{\alpha})^2 + \sum_{\alpha, \beta} \frac{1}{2} (x^{\alpha\beta})^2 \right. \right. \right. \\ \left. \left. \left. + 2n \text{Tr} \exp \left(\frac{H}{kT} \sum_{\alpha} S^{\alpha} + \left(\frac{\tilde{J}}{2\sqrt{2}kT} \right)^{1/2} \sum_{\alpha} S^{\alpha} S^{\alpha} + \frac{\tilde{J}}{kT} \sum_{\alpha, \beta} S^{\alpha} S^{\alpha} S^{\beta} S^{\beta} \right) \right] \right\} - 1 \right), \quad (2.10)$$

where the trace is now over n replicas at a single site.

For large N and integral $n \geq 2$ the integrations in (2.10) can be performed by the method of steepest descents, the integral being dominated by the region of maximum integrand. At the maximum all the x^{α} are equal as also are all the $x^{\alpha\beta}$; we denote their values by x_n, y_n . A convenient parametrization permitting analytic continuation to $n \rightarrow 0$ then follows from the substitution

$$\sum_{\alpha, \beta} \lambda_{\alpha\beta}^{1/2} S^{\alpha} S^{\beta} = \frac{1}{2} (x_n) \left[\left(\sum_{\alpha} S^{\alpha} \right)^2 - n \right], \quad (2.11)$$

together with the use of identity (2.9). With the further substitution

$$q_n = x_n (kT/\tilde{J}), \quad (2.12a)$$

$$m_n = y_n (kT/\tilde{J})^{1/2}, \quad (2.12b)$$

the integral in (2.10) for $n \geq 2$ becomes

$$\{\det A_q\}^{-1/2} \exp \left[-N \left\{ n(\bar{J}_0 m_z^2/2kT) + (\bar{J}/2kT)^2 [n(n-1)q_z^2 + 2m_z] \right. \right. \\ \left. \left. - \ln \int dz (2\pi)^{-1/2} \exp(-\frac{1}{2}z^2) (2 \cosh \bar{\Xi}_q)^n \right\} \right] (1 + O(N^{-1})), \quad (2.13)$$

where $\bar{\Xi}_q = \frac{1}{2}(\bar{J}_0 m_z + \bar{J} q_z^{1/2} z + H)/kT$, and m_z, q_z satisfy the coupled equations

$$m_z = \frac{\int dz (2\pi)^{-1/2} \exp(-\frac{1}{2}z^2) (2 \cosh \bar{\Xi}_q)^n \tanh \bar{\Xi}_q}{\int dz (2\pi)^{-1/2} \exp(-\frac{1}{2}z^2) (2 \cosh \bar{\Xi}_q)^n}, \quad (2.14)$$

$$1 = (n-1)q_z + \frac{\int dz (2\pi)^{-1/2} (\bar{J}T/\bar{J}_0)(z/q_0^{1/2})(2 \cosh \bar{\Xi}_q)^n \tanh \bar{\Xi}_q}{\int dz (2\pi)^{-1/2} (2 \cosh \bar{\Xi}_q)^n}. \quad (2.15)$$

A_q is an $\frac{1}{2}n(n-1) \times \frac{1}{2}n(n+1)$ matrix whose elements are simple functions of m and q of order unity; it is given explicitly in Appendix A. Continuing these equations to small n and substituting (2.13) into (2.10) we find

$$f = NT \left\{ \ln m_z^2/2kT + [\bar{J}^2(1-q)^2/4(kT)^2] \right. \\ \left. - (2\pi)^{-1/2} \int dz \exp(-\frac{1}{2}z^2) \ln(2 \cosh \bar{\Xi}) \right\}, \quad (2.16)$$

with

$$m = \int dz (2\pi)^{-1/2} \exp(-\frac{1}{2}z^2) \tanh \bar{\Xi}, \quad (2.17)$$

$$q = \int dz (2\pi)^{-1/2} \exp(-\frac{1}{2}z^2) \tanh^2 \bar{\Xi}. \quad (2.18)$$

Solutions of (2.17) and (2.18) may be obtained by expansion near the points $T=0$ and $T=T_g$. Before exhibiting the solutions and their consequences for the thermodynamics let us note the physical significance of m and q . As shown in Appendix B,

$$m = \langle S_1 S_2 \rangle, \quad (2.19)$$

$$q = \langle S_1^2 S_2^2 \rangle. \quad (2.20)$$

A nonzero q thus indicates magnetic order, while nonzero m (in addition to q) indicates that the order is ferromagnetic. When $m=0$ but $q \neq 0$ we call the state a spin-glass. A uniform infinite-range model does not permit periodic antiferromagnetic orderings although these are possible in related short-range interaction models.

The solution of (2.17) and (2.18) leads for $H=0$ to the phase diagram shown in Fig. 1. All the phase transition lines are second order. The phase transition from paramagnetic to ordered

magnetic state occurs at a temperature equal to the larger of $\bar{J}_0/k, \bar{J}/k$, the ordered phase being ferromagnetic if $\bar{J}_0 > \bar{J}$, spin-glass if the converse holds. A finite field H removes sharp phase transitions by allowing m and q to be nonzero at all temperatures.

For $\bar{J}_0/\bar{J} \rightarrow 1$ the effect of exchange fluctuations are weak and $q \rightarrow m^2$, in accord with the physical interpretation of q as the mean-square frozen moment per site. Although $q(T=0)=1$, $m(0)$ is diminished by weak fluctuations as

$$m(0) = 1 - (2/\pi)^{1/2} (\bar{J}/\bar{J}_0)^{1/2} \exp(-\bar{J}_0^2/2\bar{J}^2), \quad (2.21)$$

and vanishes continuously at the spin-glass phase boundary as

$$m(T) = (18\pi)^{1/2} (\bar{J}/\bar{J}_0)^{1/2} [(2/\pi)^{1/2} - \bar{J}/\bar{J}_0]^{1/2}. \quad (2.22)$$

Values of $m(T)$ and $q^{1/2}(T)$ obtained by numerical solution of (2.17) and (2.18) are exhibited in Fig. 2 for four choices of \bar{J}_0/\bar{J} . We note that the effect of fluctuations is strongest at low temperatures, causing a decrease in magnetization as $T \rightarrow 0$, and

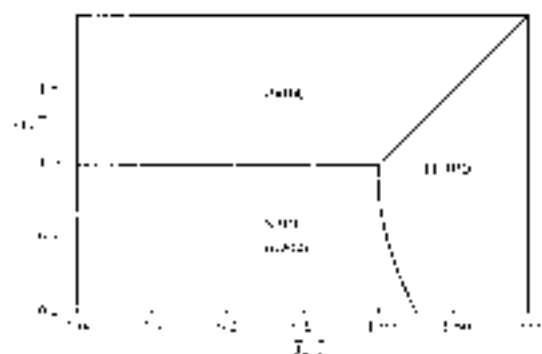


FIG. 1. Magnetic phase diagram of the random infinite-range Ising model defined by Eqs. (2.13) and (2.14), using the natural units (2.3). A spin-glass phase is obtained at low temperatures for all negative \bar{J}_0 even though the corresponding uniform system has no phase transition.

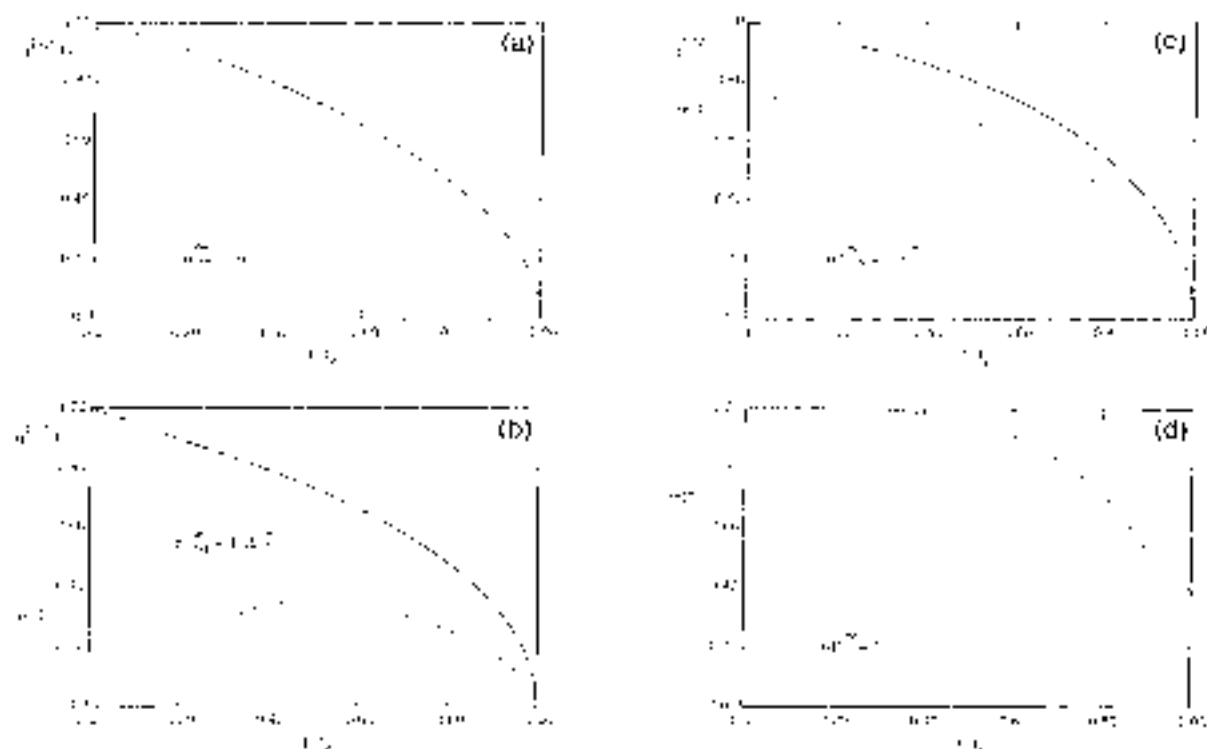


FIG. 2. Frozen moment, $q^{1/2}(T)$ (solid line), and magnetization, $m(T)$ (dotted line), for four magnetic systems described by (2), with various values chosen to represent the possibilities of the phase diagram in (1). T is scaled to the transition temperature from the paramagnetic phase to whichever ordered phase forms first. In (a), $\tilde{J}_0 = 0$, and $\alpha = 0$ for all T . In (b), $\tilde{J}_0 = 1.5\tilde{J}_c$, and the ferromagnetic phase gives way to a spin-glass phase at lower T . In (c), $\tilde{J}_0 = 1.5\tilde{J}_c$, and only a ferromagnetic phase is found, with $q^{1/2}(T)$ significantly greater than $m(T)$ for all $T < T_c$. Case (d) is a pure ferromagnet ($\tilde{J}_0 = \tilde{J}_c = 0.85q^{1/2}(T)/m(T)$).

a line of second-order transitions from ferromagnet to spin-glass with decreasing temperature for \tilde{J}_0/\tilde{J}_c between 1 and $(\frac{1}{2}\pi)^{1/2}$.

The frozen moment $q^{1/2}(T)$, as is shown in Fig. 2, is found from (2.17) and (2.18) to be proportional to $(T_c - T)^{1/2}$ just below T_c , tending to only as $T \rightarrow 0$, and is always greater than $m(T)$ at the same temperature (for $\tilde{J} \neq 0$). The low-temperature behavior of $q(T)$ is predicted to be linear:

$$q(T) \sim 1 - (2 - \pi)^{1/2} (\tilde{J}_0/\tilde{J}_c) \exp(-\tilde{J}_0/\tilde{J}_c) 2\tilde{P}(1). \quad (2.23)$$

This contrasts with the behavior of $m(T)$ in a uniform Ising system, for which all temperature derivatives vanish at $T = 0$ since excitations from the ferromagnetic ground state require a finite energy.

The standard thermodynamic functions follow straightforwardly. For example, the internal energy may be obtained via the Gibbs-Helmholtz relation, yielding

$$U/N = -[\frac{1}{2}\tilde{J}_0 m^2 + \tilde{J}^2(1 - q^2)/2\pi T + Hm]. \quad (2.24)$$

The low-temperature limit of U/N is extracted

by substituting (2.23) into (2.24). In particular,

$$U(0)/N = -[\frac{1}{2}\tilde{J}_0 m(0)^2 + Hm(0) + \frac{1}{2}\tilde{J}^2(2 - \pi)^{1/2} \exp(-\tilde{J}_0/\tilde{J}_c) m(0)^2 \tilde{P}(1)]. \quad (2.25)$$

Higher-order terms in (2.23) were calculated in order to obtain analytic expressions for the heat capacity C at low temperature. Numerical results are displayed in Fig. 3. The following features should be noted. C is zero at $T = 0$, as required by general thermodynamic considerations. At the ordering temperature, T_c , C has a singularity. If the transition is to a spin-glass, C displays a jump [Fig. 3(a)]; if the ordered phase is ferromagnetic, there is a discontinuity [Figs. 3(b)–3(d)]. In both cases, a finite contribution to $C(T)$ is found above T_c :

$$C/N \sim \tilde{J}^2/2\pi T, \quad T > T_c. \quad (2.26)$$

This latter behavior should be contrasted with the situation for a pure infinite-ranged ferromagnet (or a finite-ranged ferromagnet treated in mean-field theory) for which C vanishes above the

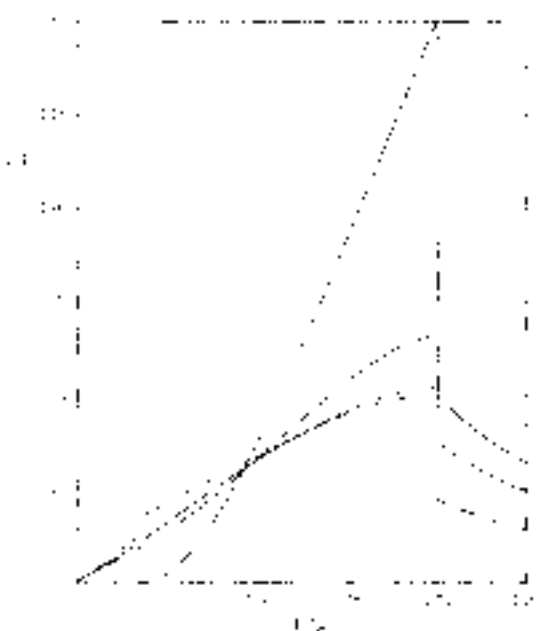


FIG. 3. Specific heat as a function of T (normalized to the relevant ordering temperature), for the four cases treated in Fig. 2: (a) $\tilde{J}_0 = 0$, solid line; (b) $\tilde{J}_0 = 1.2\tilde{J}$, short-dashed line; (c) $\tilde{J}_0 = 1.0\tilde{J}$, long-short-dashed line; (d) $\tilde{J}_0 = 0$, long-dashed line.

ordering temperature

In the spin-glass phase the leading contribution to the specific heat at low temperatures is given by

$$C/N \approx 15T^{1/2}(\tilde{J}/2\pi)^{1/2} \ln(\pi/2\pi^{1/2}) \quad (q=0), \quad (2.27a)$$

In the ferromagnetic phase, fluctuations still give rise to a linear term in C , the magnitude of which decreases to zero as $q(0)$ tends to 1 with increasing ratio \tilde{J}_0/\tilde{J} .

$$\frac{C}{N} = \left(\frac{N}{\tilde{J}}\right) \left(\frac{2}{\pi}\right)^{1/2} \left\{ \frac{1}{2} \pi - (2\pi T) \exp[-(\tilde{J}_0/\pi - \tilde{J})] \right\} \\ \times \exp[-1/2(\tilde{J}_0/\pi - \tilde{J})]. \quad (2.27b)$$

When \tilde{J}_0/\tilde{J} lies between 1.0 and $e^{1/2} \approx 1.25$, the transition from spin-glass to ferromagnet with increasing temperature is induced by a second discontinuity in $C(T)$. This case is shown in Fig. 3(b).

The susceptibility χ at general H may be obtained directly from (2.15) and has been illustrated for various cases within the spin-glass parameter range in Fig. 3 of Ref. 3. In the limit $H=0$ the susceptibility may be simply expressed in terms of q as

$$\chi(T) = [1 - q(T)^{-1/2} T - \tilde{J}][1 - q(T)] \\ \chi^{-1} = (1 - \tilde{J})\chi^{-1(0)}, \quad (2.28)$$

where $\chi^{-1(0)}$ is the result for $\tilde{J}=0$. Above the ordering temperature, where $q=0$, this is just a Curie-Weiss law. In the spin-glass phase, fluctuations decrease $\chi^{-1(0)}$ and χ , giving rise to a sharp positive \tilde{J}_0 enhances χ at all temperatures.

Within this formulation the entropy is given by

$$S/N = -[\tilde{J}/m] \{ 2\pi + (\tilde{J} - 4\pi T^2)(1 - q)(1 - 3q) - 4\pi \} \\ - k[2\pi T^{1/2} \int_0^\infty dx \exp(-x^2/2) \ln(2 \cosh x)]. \quad (2.29)$$

At high temperatures this yields physical results, which we shall see are in accord with series expansions, but it leads to unacceptable consequences as $T \rightarrow 0$, for example if $H=0$, $m=0$, the $T=0$ limit of (2.28) is $-\infty$. This incorrect result is the most obvious indication that the procedure used above of employing integration $\rightarrow 2$ results to small contributions is not correct in all details as T tends to zero. Other evidence lies in the computer simulations reported below. On the other hand, the computer simulations verify many of the qualitative features below the ordering temperature. Both the simulations and partial summations of high-temperature series indicate that the results for temperatures greater than the ordering temperature are correct, as also is the prediction of that temperature.

Another apparent difficulty is that f of (2.16) cannot be established a functional variational free-energy function. Although it has an extremum at $q(0)$ as given by (2.17), (2.18), this extremum is not a minimum in the spin-glass phase but a maximum.¹¹ This particular difficulty does not invalidate the solution since f is not such a variational function but rather is defined only at the physical values of q, m . In particular it is evident from series expansions (see Sec. III) that the spurious minimum of f at $q=0$ (and, say, for $H=0$, $\tilde{J} < \tilde{J}_0$) does not represent a stable solution.

Finally, by way of further support for aspects of the above analysis, it should be noted that since the preliminary report of this work the spherical model analogue of (2.3), (2.4), and (2.6) has been solved at all temperatures by Kosterlitz *et al.* They use two methods of analysis: the $\epsilon \rightarrow 0$ procedure, and a direct method, not generalizable to the Ising model, which employs the exact eigenvalue spectrum of a Gaussian random infinite matrix. They find the same results by both procedures, provided care is taken in the order of certain multiple integrations. The spherical model

also gives a negative entropy at $T = 0$ but this is general for classical equilibrium models. They do, however, also find that ρ is maximized for the spin-scalar q in the $n \rightarrow 0$ limit. These results give us extra confidence in the general nature of the $n \rightarrow 0$ procedure.

III. HIGH-TEMPERATURE SERIES

In our preliminary letter it was noted that the specific heat above the ordering temperature as derived above is identical with that given by high-temperature series expansions. In fact, however, as noted by TAP, the high-temperature series for the free energy F of the model given by (2.3) in (2.4) can be summed completely at least to order N^{-1} without using any $n \rightarrow 0$ tricks giving (i) the same results as above for $kT \gg J$ and \tilde{J} and (ii) no expansion at temperatures equal to the transition $\tilde{J} = kT$ and $\tilde{J} = kT$. This means that the series for the free energy then plays a role in our calculations and correctly gives in Sec. III a transition which is continuous or weaker than spin-glass. Below is a sketch of the calculation for the free Hamiltonian of (2.5) with $H = 1$.

Using standard manipulations, the partition function may be expressed as

$$Z = \text{Tr} \prod_{i,j} \exp(-K_{ij} S_i S_j) \quad (3.1)$$

$$= \sum_{\{S_i\}} \left(\prod_{i,j} \exp(K_{ij} S_i S_j) \right) \prod_{i,j} (1 + S_i S_j J_{ij}) \quad (3.2)$$

where

$$K_{ij} = J_{ij} + kT \quad (3.3)$$

$$J_{ij} = \text{tr}(K_{ij} S_i S_j) \quad (3.4)$$

The normalized free energy is therefore given by

$$\begin{aligned} F &= -kT \ln Z = -\frac{kT}{N} \sum_{i,j} \int_0^1 d\alpha P(\alpha) \int_0^1 d\beta P(\beta) \text{tr}(\exp(K_{ij} S_i S_j)) \\ &= -\frac{kT}{N} \int_0^1 \int_0^1 d\alpha d\beta \sum_{i,j} P(\alpha) P(\beta) \\ &\quad \times \ln \left(2^{-N} \text{tr} \prod_{i,j} (1 + S_i S_j J_{ij}) \right) \quad (3.5) \end{aligned}$$

1

Diagrammatically the argument of the log in the last term of (3.5) is the sum of closed loop diagrams with an even number of bonds at each vertex and no repeated bonds. Repeated bonds can occur once the logarithm is expanded. Taking the average against $P(\tilde{J}_{ij})$ given by (2.4) with the scalings (2.8), one retains to order N^2 in the last term of (3.5) only single and double polygons. One finds

$$\begin{aligned} F &= -kT \ln 2 - \tilde{J}^2/4kT - kT/2N \ln(1 - \tilde{J}/kT) \\ &\quad - kT/2N \ln(1 - \tilde{J}^2/kT^2) - \tilde{J}_2/2N + O(N^{-1}), \quad (3.6) \end{aligned}$$

where the \ln strictly signifies the first N^{-1} terms of the expansion of the logarithm. From (3.6) we can make the following: (i) for $kT \gg \max(\tilde{J}, \tilde{J}_2)$ the free energy is given to leading order by

$$F = -kT \ln 2 - \tilde{J}^2/4kT, \quad (3.7)$$

in agreement with (2.16) and (ii) the series diverges at $kT = \max(\tilde{J}, \tilde{J}_2)$, signalling the transition to the paramagnetic phase at the same temperatures as obtained in Sec. II. Below this temperature, the paramagnetic phase is unstable. When the single bond polygon series is divergent, one expects a transition to a phase in which $\langle S_i S_j \rangle$ is nonzero, while a divergence of the double-bond polygon series is consistent with nonvanishing $\langle S_i S_j S_k S_l \rangle$. These observations are in agreement with the rest of part of the phase diagram (Fig. 1) predicted by the replica theory.

IV. OTHER INFINITE-RANGED SPIN GLASS MODELS

Equation (2.2) can be generalized to give a Hamiltonian for general classical n -vector spin glasses in the form

$$H = \sum_{i,j} J_{ij} \tilde{S}_i \cdot \tilde{S}_j + \tilde{h} \cdot \sum_i \tilde{S}_i, \quad (4.1)$$

with $P(d_{ij})$ a continuous distribution as before. We believe that this model is in principle solvable for arbitrary n , and give below a solution for the planar model ($n = 2$). We shall use the $n \rightarrow 2$ limiting procedure.

With the transformations as employed for the Ising problem the free energy for an arbitrary n -vector model may be expressed as

$$F = -kT \lim_{n \rightarrow 2} \lim_{N \rightarrow \infty} \ln \left(\frac{1}{N} \text{tr} \exp \left[\sum_{i,j} \left(\frac{J_{ij}}{N} \sum_{\alpha} \tilde{S}_i^{\alpha} \tilde{S}_j^{\alpha} + \frac{\tilde{h} \cdot \tilde{S}_i}{N} \sum_{\alpha} \tilde{S}_i^{\alpha} \right) \right] \right), \quad (4.2)$$

For the plaquette model this can be put into a form suitable for steepest descents analysis using

$$\cos(\varphi_1^{\alpha\beta} - \varphi_2^{\alpha\beta}) = \cos(\varphi_1^{\alpha\beta} - \varphi_1^{\beta\alpha}) \\ \frac{1}{2}(\vec{S}_1^{\alpha\beta} \cdot \vec{S}_2^{\alpha\beta} + \vec{T}_1^{\alpha\beta} \cdot \vec{T}_2^{\alpha\beta}), \quad (4.3)$$

where $\vec{S}_i^{\alpha\beta}$ is a two-dimensional unit vector characterized by an angle

$$\varphi_1^{\alpha\beta} = \varphi_1^{\alpha} + \varphi_1^{\beta}, \quad (4.4)$$

and $\vec{T}_i^{\alpha\beta}$ is a similar unit vector with the angle

$$\varphi_1^{\alpha\beta} = \varphi_1^{\alpha} - \varphi_1^{\beta}. \quad (4.5)$$

For $\alpha = 1$, $\vec{T}_i^{\alpha\beta}$ reduces to \vec{U}^{β} , a unit vector oriented at an angle $2\varphi_1^{\beta}$. With this notation, f may be rewritten

$$f = -kT \lim_{N \rightarrow \infty} \lim_{q \rightarrow 0} (qN)^{-1} \left\{ \text{Tr}_\sigma \exp \left[\frac{J_0}{2kT} \sum_\alpha \left| \sum_i \vec{S}_i^\alpha \right|^2 + \frac{J^2}{8(kT)^2} \sum_{\alpha\beta} \left(\left| \sum_i \vec{S}_i^{\alpha\beta} \right|^2 + \left| \sum_i \vec{T}_i^{\alpha\beta} \right|^2 \right) \right] \right. \right. \\ \left. \left. + \frac{J^2}{8(kT)^2} \sum_{\alpha\beta} \left| \sum_i \vec{U}_i^\alpha \cdot \vec{U}_i^\beta \right|^2 + \frac{J^2}{2kT} \sum_{\alpha\beta} \left(\frac{J_0}{8(kT)^2} (qN - 2Nq) \right) \right] - 1 \right\} \quad (4.6)$$

$$= -kT \lim_{N \rightarrow \infty} \lim_{q \rightarrow 0} (qN)^{-1} \left\{ \exp(\tilde{J} q N / 8kT)^2 \int \prod_\alpha (N/2\pi) d\alpha^\alpha d\alpha^\beta \prod_\alpha (N/2\pi) d\alpha^{\alpha\beta} d\alpha^{\beta\alpha} \right. \\ \times \exp \left\{ -N \left[\sum_\alpha \left(\frac{1}{2} |s^\alpha|^2 + \frac{1}{2} |s^\beta|^2 \right) + \sum_{\alpha\beta} \left(\frac{1}{2} |s^{\alpha\beta}|^2 + \frac{1}{2} |s^{\beta\alpha}|^2 \right) \right. \right. \\ \left. \left. + \ln 2\pi \exp \left(\sum_\alpha \left[(\tilde{J}_0/kT)^{1/2} \vec{S}^\alpha \cdot \vec{S}^\alpha + (\tilde{J}/2kT) \vec{S}^\alpha \cdot \vec{U}^\alpha \right] \right. \right. \right. \\ \left. \left. \left. + (\tilde{J}/2kT) \sum_{\alpha\beta} \left(\vec{S}^{\alpha\beta} \cdot \vec{S}^{\alpha\beta} + \vec{U}^{\alpha\beta} \cdot \vec{U}^{\beta\alpha} \right) \right] \right] \right\} \right\}. \quad (4.7)$$

the trace is taken over spins at a single site only. This integral can be performed by steepest descents as was done for the Ising model in Sec. II.

The general steepest descents treatment is complicated. We therefore make the physical Ansatz that for small enough \tilde{J}_0 there exists a spin-glass extremum with $s^\alpha = s^\beta = s^{\alpha\beta} = 0$ and with all the $|s^{\alpha\beta}|$ equal. The angle of $\vec{S}_{\alpha\beta}$ in its reference plane is

arbitrary. We set it to zero for convenience. Anticipating this identification of the order parameter in the limit $q \rightarrow 0$, we define

$$q_r = q^{(r)} = |s^{\alpha\beta}|^2 2kT/\tilde{J} \quad (4.8)$$

at the extremum. The trace in (4.7) may now be expressed as

$$\text{Tr} \exp \left((\tilde{J}/2kT)^{1/2} q_r \sum_{\alpha\beta} \cos(\varphi^\alpha - \varphi^\beta) \right) \int \prod_\alpha \frac{d\varphi^\alpha}{2\pi} \int \frac{d\tilde{\varphi}}{2\pi} \exp(-1/2) \exp \left(\frac{\tilde{J}}{kT} \left(\frac{1}{2} q_r \right)^{1/2} \tilde{\varphi} + \sum_\alpha \xi^\alpha \right) \exp \left[-n q_r \left(\frac{\tilde{J}}{2kT} \right)^2 \right], \quad (4.10)$$

where the φ integration is two dimensional and leads to

$$\int_0^{2\pi} \int_0^{2\pi} \varphi d\varphi \exp \left[-\frac{1}{2} \varphi^2 (n \tilde{J}_0 \tilde{J} / 2kT) + \frac{1}{2} q_r \varphi^2 \right] \exp \\ \times \exp[-n q_r (\tilde{J}/2kT)^2], \quad (4.11)$$

where

$$I_n(x) = \int_0^{2\pi} \int_0^{2\pi} (d\varphi/2\pi) (\cos \varphi)^n e^{i\varphi x} \quad (4.12)$$

is a modified Bessel function of n th order.

Applying the extremal condition to (4.7) and tak-

ing the limit $x \rightarrow 0$ we obtain

$$q = 1 - (kT/\tilde{J})(2/q)^{1/2} \\ \times \int_0^{\infty} x \, dx \exp(-\frac{1}{2}x^2) \frac{I_1[\frac{1}{2}(x/q)^{1/2}/kT]}{I_0[\frac{1}{2}(x/q)^{1/2}/kT]}. \quad (4.13)$$

This yields a spin-glass ordering temperature $T_g = J/2k$, as compared with J/k for the Ising case and $\tilde{J}/3k$ found for the Heisenberg system by Edwards and Anderson. We speculate that for an m -vector classical model there will be a second-order spin-glass transition at $\tilde{J}/m\sqrt{2}$. Below the ordering temperature, q increases as

$$q = 1 - O(T^2), \quad (4.14)$$

where $x = (T_g - T)/T_g$. At low temperature, q approaches unity linearly in T :

$$q = 1 - \tau^{1/2}/(kT/\tilde{J}) + O(T^2). \quad (4.15)$$

The free energy is given by

$$f = -(\tilde{J}^2/8kT)(1 - q)^2 \\ - \int_0^{\infty} x \, dx \exp(-\frac{1}{2}x^2) \ln_{10}[\tilde{J}x/(q)^{1/2}/kT], \quad (4.16)$$

and the internal energy by

$$U = -(\tilde{J}^2/4kT)(1 - q^2). \quad (4.17)$$

This leads to a specific heat which tends to a constant $1/k$ per spin, at $T = 0$, a consequence of the classical nature of the system. It has a cusp at the usual sort at T_g , and decreases as $\tilde{J}^2/4kT^2$ above T_g .

V. MONTE CARLO TESTS OF THE THEORY

The infinite-ranged interactions that make it possible to demonstrate the existence of a spin-glass transition in the model Hamiltonian (1.1) do not occur in nature. In order to test the predictions of the present replica methods or the extended mean-field theory of TAP for the low-temperature phase, the necessary experiments were performed by computer simulation. Data obtained in samples of up to 400 spins are reported and compared with theory in this section. Since space and time constraints limited the sample size N to a relatively small number of spins ($N < 800$), some attention is given to determining the dependence of the results on N .

Since the replica method predicts an unphysical (slightly negative) entropy in the limit $x \rightarrow 0$, we have made a fairly extensive study of the ground-state properties of the infinite-ranged Ising spin-glass as a function of \tilde{J}_0 and compare these with the other predictions of the theory in Fig. 4-6.

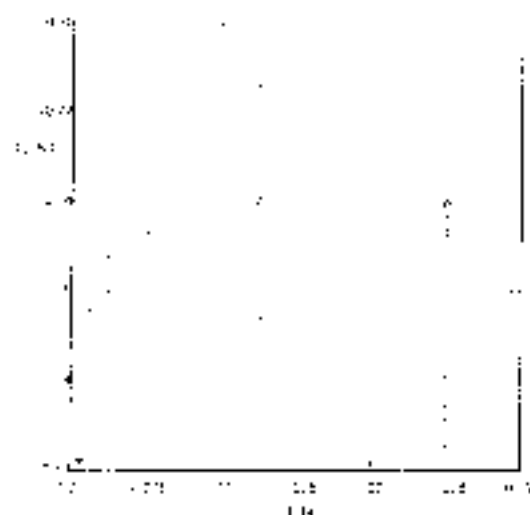


FIG. 4. Ground state energies found for finite samples with interactions coupled to all pairs of spins, calculated as in (4.2), with zero field. For each size, N , 100 realizations of samples stored away; 40 spins = 4000 samples; 80, 1600; 160, 600; 320, 150; and 640, 40. The curve indicates the ground-state energy prediction, (4.1), for an infinite sample.

The TAP analysis¹ is confined to the case $\tilde{J}_0 = 0$, and differs significantly from the present work only for $T > 2.5 T_g$. We compare Monte Carlo results with the predictions of the two theories, emphasizing the low-temperature results in Figs. 7-11.

In order to obtain predictions for the low-tem-

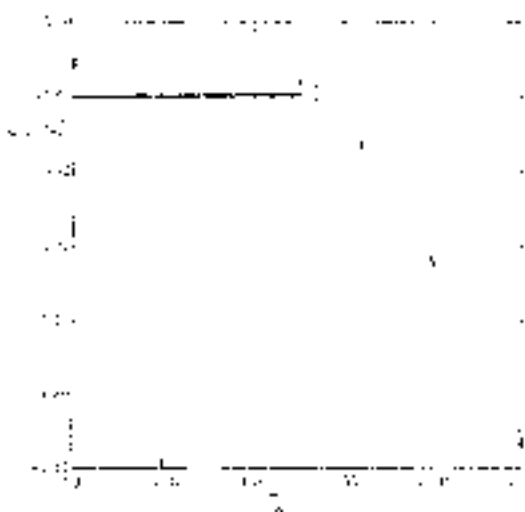


FIG. 5. Ground state energies E/NkT , for 400-spin samples, as a function of \tilde{J}_0 ; each point represents an average over 20 cases. The solid line theories of the spin-glass phase or the predicted result (4.17).

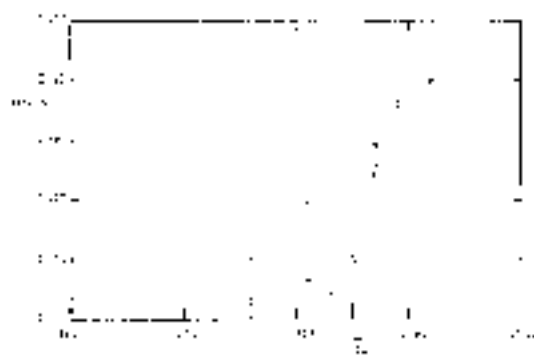


FIG. 6. Zero-temperature magnetization for 500-spin samples in an applied field $h = 0.01J$. Data points represent average and error variations found in 25 cases at each value of J_1 .

perature thermodynamics, TAP characterize the low-energy excitations of a spin-glass by a distribution of single-spin molecular fields $\{h_i\}$ neglecting possible excitations which might require the simultaneous reversal of more than one spin. They argue that such a distribution is only stable against further spin rearrangements if $\rho(h)$ increases from zero no faster than linearly in h at small fields. [A related argument has been used to show that $\rho(E) = 0$ for random exchange interactions which decay as $1/R^3$; see Ref. 18.] This implies that $q(T) = 1 + \alpha(hT/\Delta T)$, instead of the linear T de-

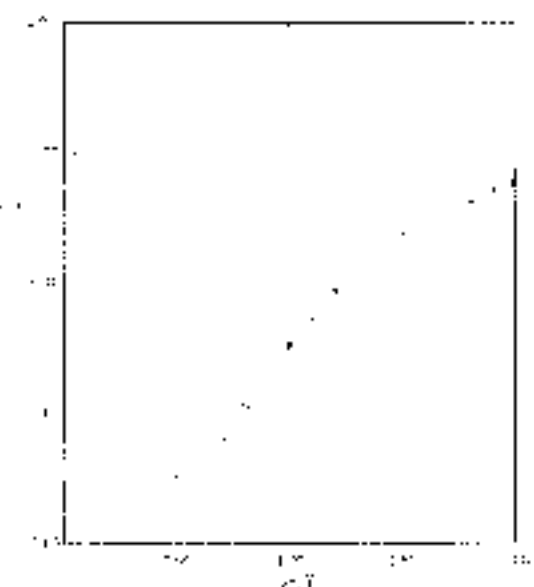


FIG. 7. Internal energy as a function of $1/T$ for four samples, 500 spins each. Error bars on the points at $hT = 0.1, 0.5J$, and $1.0J$ indicate typical standard-to-standard variations. The solid line gives the prediction of the replica theory.

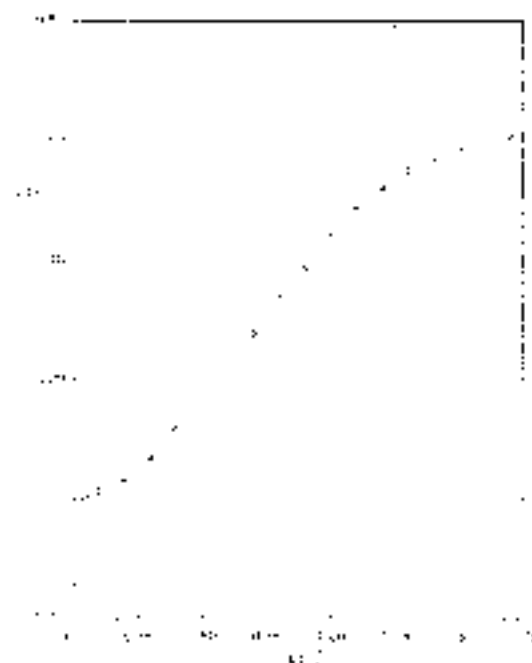


FIG. 8. Entropy as a function of temperature, obtained by integrating the Monte Carlo data of Fig. 7 (data points), and as predicted by the replica theory (solid line). The Monte Carlo results remain positive at all temperatures, and are in good agreement with the TAP prediction (dashed line) at low temperatures.

pendence given by (2.23). TAP suggest that α should be the value which gives the maximum density of low-energy excitations consistent with their mean-field equations, $\alpha = 2(\ln 2)^{-1} = 1.665$,

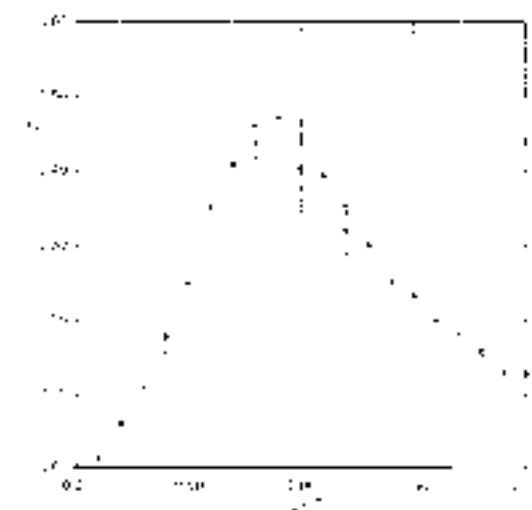


FIG. 9. $C(T)/T$, averaged over four samples of 500 spins each, with $J_1 = 0.0$. The solid line gives the replica theory result, which is linear in T as $T \rightarrow 0$. The dashed line indicates the TAP prediction.

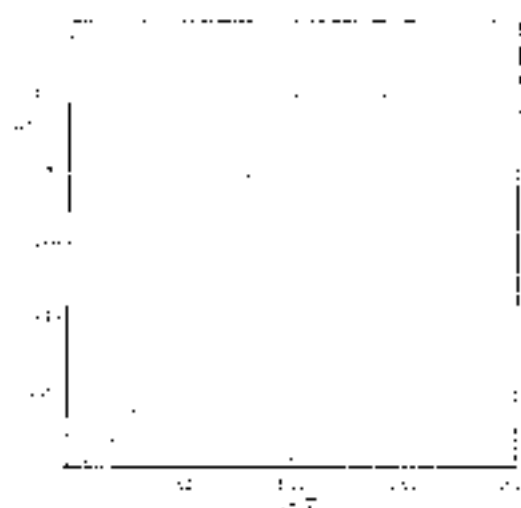


FIG. 10. $E(0)$, averaged over five samples of 500 cases each, with $\beta_1 = 1.0$. The solid and dashed lines give the replica theory and TAP predictions, respectively.

Once α is determined, predictions are readily obtained for $\chi(T) = \alpha(\partial F/\partial T)$, $S(T) = (1/\alpha)(\partial F/\partial T)^2$, and $C(T) = (1/\alpha^2)(\partial^2 F/\partial T^2)$.

Some of the glassy features found in actual spin-glasses,¹ such as the existence of many metastable energy minima and unusual slow relaxation phenomena, also occur in the computer simulations and can be subjected to "microscopic" examination. We report preliminary results of such a study below.

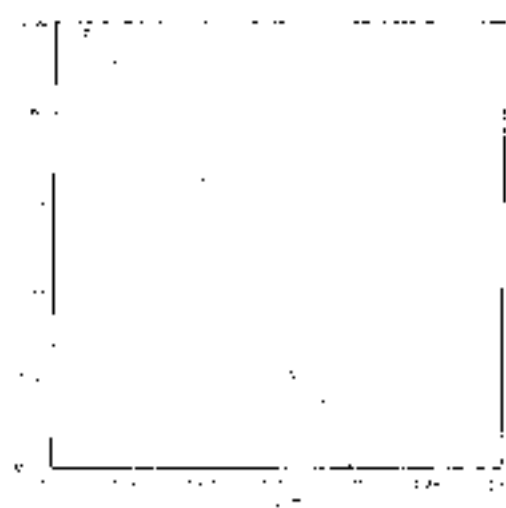


FIG. 11. Edwards-Anderson order parameter $q(T)$, obtained from the data of Fig. 10. Averages were taken over 400 time steps per spin at each temperature. Solid and dashed lines are replica theory and TAP results.

The simplest property to test is the internal energy. Specializing (2.25) to the spin-glass phase gives

$$E(0)/JN = -12/\pi^{1/2} \approx -0.70. \quad (5.1)$$

We wish to check two features of (5.1)—first, that $E(0)$ scales as J (i.e., as $N^{1/2}$), and second the value of the coefficient. One can construct upper bounds to $E(0)$ which show that $E(0)/JN$ must be extensive. Consider the following "dynamic programming" construction of an approximate ground state: The spins are arbitrarily numbered $1-N$. The alignment of spin 1 is arbitrary. The orientation of spin 2 is chosen to make $J_{12}S_1S_2 \leq 0$ so that the contribution $E_{12} = J_{12}S_1S_2$ to the internal energy is negative. The orientation of spin 3 is then chosen to make $E_{13} = J_{13}S_1S_3 \leq 0$, and so forth. The internal energy of the approximate ground state constructed in this way is obtained by summing all the E_{ij} , and gives an upper bound to the actual $E(0)$. The average value of E_{ij} is $-J(2/\pi)^{1/2}$, and that of E_{1i} is $-J(2\alpha/\pi)^{1/2}$. The expectation value of the sum of all contributions gives the bound

$$\frac{E(0)}{JN} \leq -\left(\frac{2}{\pi}\right)^{1/2} N^{-1/2} \sum_{i=1}^{N-1} n^{1/2} = -\frac{2}{3} \left(\frac{2}{\pi}\right)^{1/2} \approx -0.63, \quad (5.2)$$

which is $\frac{1}{3}$ of the replica prediction.

A fairly elaborate procedure was followed in the calculations to ensure accurate estimates of $E(0)$ for finite samples. The heuristic precautions described below were taken because the computational effort necessary to prove that no better ground state exists increases rapidly with increasing N . Attempts to improve upon the bound (5.2) by constructing the m lowest-energy configurations of $n+1$ spins, and so forth, proved ineffective. For $N=100$, keeping track of the lowest 100 states as each spin was added gave no significant improvement over (5.2). Only for samples with fewer than 50 spins were apparently convergent estimates obtained, and this required keeping track of 2000 or more intermediate configurations. In the language of computational complexity theory,¹² finding the ground state of a spin-glass has features in common with the "NP-complete" problems, which always require $\exp(N)$ effort to solve in the worst case. What is surprising is that all samples prove to be "worst cases."

For each sample, many random starting arrangements of spins were constructed, and for each starting configuration a deterministic procedure, analogous to the method of steepest descent, was followed to reach a minimum energy. At each step a list of partial exchange energies

$\sum_j J_{ij} S_i S_j$ is constructed. The spin with the highest energy is flipped (if that energy is positive), and the list corrected. If no spin can gain energy by flipping, pairs of spins are searched to find a pair which will lower the energy of the system if they flip simultaneously. If such a pair is found they are flipped and the search over single spins continues. If not, selected triples and quartets of spins with small individual exchange fields are also searched. Such searches were carried out for 60–80 starting configurations in each Monte Carlo sample, keeping the best ground state encountered. Small further improvements to the ground-state energy were obtained by slightly disordering the best ground states ("warming" them to a temperature 2 or 3 times T_c for a few time steps per spin) and repeating the descent procedure.

The data obtained, plotted in Fig. 4, confirm that the ground-state energy scales as \bar{J} , the central feature of the Edwards-Anderson picture. However, the coefficient given in (5.1) lies below the values actually found in samples of 40–300 spins, and the discrepancy appears to be outside the range of possible error. Fig. 4 suggests that the calculated $f(0)/J_N$, extrapolated to infinite sample size, must lie somewhere between -0.75 and -0.77 . This agrees with the -0.755 ± 0.01 which VAP report from their Monte Carlo calculations. The replica theory predicts too low a ground-state energy [since the negative entropy implies $dF(T)/dT > 0$ as $T \rightarrow 0$], but the magnitude of the discrepancy is only $3\% - 5\%$.

Various portions of the descent algorithm were used on four 500-spin samples with $\bar{J} = 0$ to determine their relative efficiency. The lowest energies obtained using only single spin flips and 80 random starting configurations of spins ranged from -0.71 to -0.74 . Searching also for spin pairs which could flip narrowed this range to -0.72 to -0.74 by lowering the higher-energy states. The further improvement from considering three and four-spin processes was of order 0.001. The warmup process made a more significant contribution. The samples were warmed briefly to $3T_c$, then relaxed into the ground state, then warmed to $1.5 T_c$ and cooled, and finally warmed to $0.75 T_c$ and cooled. After this process, all four were found to have minimum energies between -0.75 and -0.76 .

The discrepancy between Monte Carlo results for $f(0)$ and the prediction (2.25) decreases with increasing \bar{J} , as is seen in Fig. 5. Although (2.25) predicts that $f(0)$ is independent of \bar{J} , in the spin-glass phase, since $q(0)$ and $u(0)$ are, the calculations show $f(0)$ decreasing slightly as the ferromagnetic phase is approached. There is no evidence for a discontinuous change in the derivative

of $f(0)$ with respect to \bar{J} at the phase boundary in agreement with (2.25). (There does appear to be a discontinuous change in slope in the $f(0)$ data¹⁰ obtained on finite-dimensional spin-glasses with the bonds restricted to take the values $\pm J_0$.)

More direct evidence of the spin-glass ferromagnet phase boundary is shown in Fig. 6, which compares the observed ground-state magnetization (in a small external field) with the predictions of (2.21) and (2.22). Very large fluctuations in the magnetization, both from sample to sample and between different low-energy states of a given sample, were observed for $1.0 < \bar{J} < 1.4$. The predicted phase boundary occurs at $a^{1/2} = 1.25$, the concentration which in fact shows the largest scatter in $m(0)$. The fluctuations seen in Fig. 6 have a parallel in the recent observation by Vannimenus and Toulouse¹¹ that (for two-dimensional Ising models with interactions of random sign but uniform magnitude) the energy cost of forming a domain wall around a region of reversed spins becomes very small close to the spin-glass ferromagnet phase boundary. For $\bar{J} = 1.5$, agreement between theory and experiment in Fig. 6 appears excellent.

VI. SPIN GLASS FOR $\bar{J} > 0$

To study the properties of an infinite-range spin-glass at finite temperatures, we have performed Monte Carlo simulations on four samples of 500 spins, each with $\bar{J} = 0.0$, taking data at temperatures from zero to $2T_c$. These are described below and compared with the predictions of Sec. II. Within the replica treatment, thermodynamic properties are independent of \bar{J} , in the spin-glass phase, since \bar{J}_0 enters Ξ only when multiplied by $u(T)$, which is zero, so study of this one set of samples would seem sufficient to characterize the phase. However, the ground-state energies plotted in Fig. 5 show that some properties may be modified sufficiently close to the ferromagnetic phase boundary.

The calculations were performed by starting each system in its lowest known energy state, and letting each sample evolve for 400 time steps per spin as an ascending series of temperatures. The data plotted in Figs. 8–10 were obtained by averaging over the last 200 time steps at each temperature. The results were compared with averages over larger and smaller time intervals to ensure that equilibrium was reached. The error bars on selected data points in Figs. 8–10 indicate the variation from sample to sample (rms deviation). Some Monte Carlo runs with larger or smaller samples, or much longer averaging times were also performed as checks.

The internal energy $\epsilon(T)$ obtained in this way is compared with the prediction of (2.18) and (2.24) in Fig. 7. The discrepancy seen at $T=0$ in Figs. 5 and 6 persists up to roughly $0.5 J_F$. The Monte Carlo observations at T_c and above agree with the theory to within numerical uncertainty. The entropy has been obtained by integrating $T^{-1}d\epsilon(T)$ up to $2J_F$, using the data in Fig. 7, and matching to the high-temperature limit, $S \sim \ln 2 - J^2/4kT^2$, of (2.20). Figure 8 compares the computed entropy with the result of substituting the solution to (2.16) into (2.29), and with the TAP low-temperature prediction.

$ST_c \approx 0.152 - 1/4$ as predicted. The magnetic entropy extracted at temperatures above T_c in the present model is therefore less than as observed experimentally,^{1,2} or in calculations on finite-dimensional spin-glass models.^{2,11} Below $\approx 2.5 T_c$, agreement between Monte Carlo and the replica theory becomes poor. The entropy predicted by (2.29) goes negative at $T \approx 0.25 J_F$, while the computed $S(T)$ appears to go to zero with zero slope. The TAP T^2 dependence and coefficient gives a good account of the Monte Carlo entropy for $T > 0.5 J_F$.

This behavior for $S(T)$ is consistent with a specific heat which increases from zero no faster than as T^2 . In Fig. 9 are plotted the Monte Carlo results for $C(T)$, obtained by averaging energy fluctuations over the final 280 time steps out of 400 at each temperature. The results agree fairly closely with the theory (2.28) above T_c , but lie consistently below the prediction of (2.25) for $T < T_c$. Figure 9 suggests that at low temperatures, $C(T)$ tends to zero with zero slope and in qualitative agreement with TAP, but the data are too crude to distinguish $C \propto T$ from an activated form, $C \propto \exp(-U/T)$, such as is found in conventional Ising ferromagnets. Similarly, $\chi(T)$, obtained by averaging

$$\chi(T) = N^{-1} \left(\sum_i S_i^2 \right), \quad (5.3)$$

is plotted in Fig. 10. It is found to be ≈ 1 above T_c , and lies below the prediction of (2.28) when $T < T_c$. The disagreement would be more striking if $\chi(T)$ were plotted. Equation (2.28) gives $\chi(T) = (2/\pi)^{1/2}$ as $T \rightarrow 0$, while the Monte Carlo results are consistent with $\chi(0) = 0$.

The differences between simulations and the replica theory in both Figs. 9 and 10 can be summarized by saying that the system appears to be more ordered than the theory would predict. Figure 11, which shows results for $q(t)$ as directly calculated using (2.26) from the simulations, confirms this trend. We see that $q(t)$ lies consistently above the value obtained from (2.16). In both Figs. 10 and 11, the TAP expressions give a good account

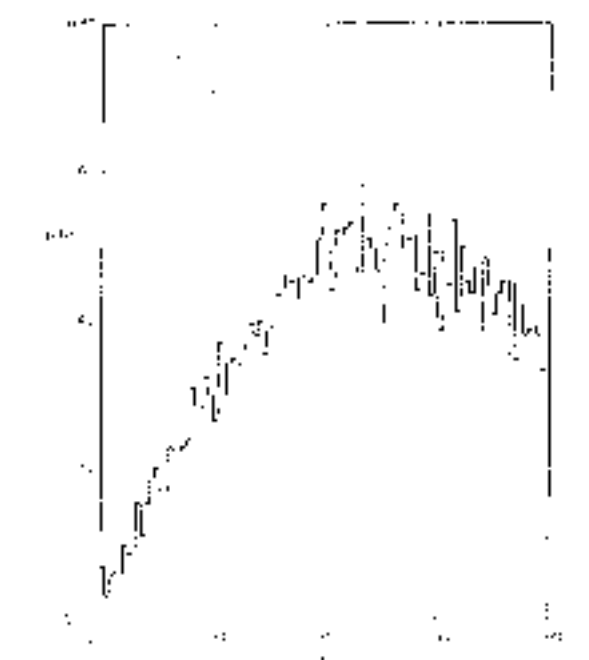


FIG. 12. Distribution of partial exchange energies $p(b)$ as defined in (5.1), averaged over all samples of 900 spins each, with $J_F = 0.5$. The dashed line indicates the MRF prediction $\tilde{p}(b)$.

of the low-temperature data.

In the course of the ground-state and Monte Carlo calculations, the one-spin excitation energies,

$$h_i = \sum_j J_{ij} S_j S_i, \quad (5.4)$$

are available and can be used to test TAP's conclusions about $p(b)$ as well as the assumptions of mean-random-field (MRF) treatments of the Marshall-Klein-Brook^{23,24} type, which attempt to construct a self-consistent $p(b)$. The distribution $p(b)$ found in the ground states of twenty 300-spin samples, the largest size studied, is plotted in Fig. 12. As TAP predicts, $p(b)$ is linear to b for small b . The small positive intercept appears to be an artifact of the finite sample size, and decreases slowly with increasing N .

Mean-random-field theories predict a $p(b)$ which is qualitatively unlike the results in Fig. 12. The major difficulty is that such theories when applied to Ising systems invariably give $p(0) = 0$. For the infinite-ranged model, Klein has proposed²⁵ that the appropriate MRF is

$$p(b) = (2/\pi)^{1/2} (q^{1/2} \exp(-b^2/2J^2/q)), \quad (5.5)$$

arguing that (2.17) and (2.16) should be interpreted as self-consistent equations of the MRF type, viz.,

$$\langle h_i^2 \rangle = \int db \tilde{p}(b) \langle \text{anh}(bq) \rangle, \quad (5.6)$$

We plot (5.5) in Fig. 12 as a dashed line, and ob-

serve that it bears no special resemblance to the observed distribution. The disagreement is most obvious at small δ . Within the MRF approximation one can calculate the internal energy from $p(\delta)$ by

$$U(T) = -\frac{1}{2} \int d\delta p(\delta) \delta \tanh(\beta\delta). \quad (5.7)$$

However, this predicts a ground state energy $U(0)/JN = -(2\pi)^{1/2}/\pi$, which is half of the replica theory result, and far from the actual value observed in the simulations (Fig. 4). The identification of the factor $\exp(-v)$ in (2.17) as a Gaussian MRF is therefore inconsistent with the thermodynamics of (2.16).

Some of the microscopic details accessible during a computer simulation do not have direct experimental consequences but are nonetheless useful guides to one's intuition. One possibility we explored during the simulations was determining the number of distinct ground states of some samples and searching for the activation pathways which connect them. Two ground states were deemed distinct if their energies differed by more than $0.0001 \sqrt{J}$. Using the deterministic descent procedure described above we first counted the number of distinct local minima found by starting from many randomly generated initial spin configurations in samples with $N = 20, 30, 40$, and 100 spins (20 samples each). The number of ground states reached was: ($N = 20$) 2.6; ($N = 30$) 8.45 \pm 3.5; ($N = 40$) 25.0 \pm 6.5; and ($N = 100$) 415 \pm 19. For the smaller sample sizes, 400 starting configurations were used. For the $N = 100$ samples, after 2000 trials only one or two new local minima were being encountered every 50 trials. Therefore, while in principle the ground numbers represent lower bounds to the actual number of energy minima, we do not expect large errors.

One might think of the phase space of a spin-glass as consisting of large valleys separated by high activation energies, each valley containing many local minima. The large activation barriers between valleys represent the reversal of large clusters of spins, which will either require high energy or have low entropy (since many spin flips must be coordinated), and thus is an extremely rare event in thermal equilibrium. The local minima are separated by reversals of one or a few spins, which can involve relatively low activation energies. To test this view we started each sample in its lowest-energy state and allowed it to evolve by the usual Monte Carlo dynamics at a constant temperature T while sampling with the descent algorithm for local minima. After each descent, time evolution was resumed from the configuration at temperature T from which the descent was taken. For $T = 2T_g$, this process yields many fewer distinct minima than did sampling from ran-

domly generated configurations.

To estimate the number of valleys as a function of N , we divide the average number of minima found by searching at $T = T_g$ into the total number of minima found for that sample. The results are: ($N = 20$) 1; ($N = 30$) 2.2; ($N = 40$) 3.5; and ($N = 100$) 13.6. Both the total number of ground states and the number of valleys appear to increase as some small power of N , rather than as $\exp(N)$, consistent with our finding in Fig. 8 that $S(0) = 0$. Since the passes connecting two valleys are apparently inaccessible at T_g and lower temperatures, this picture of the low-temperature states of a spin-glass provides a possible starting point for thinking about remanence and other "glassy" experimental phenomena.

VII. DYNAMICS FOR $T > 0$

Study of the dynamical properties of spin-glass models of with infinite-ranged interactions shows additional differences between the spin-glass and conventional ferromagnets. In particular, the behavior of the systems in their low-temperature phases proves to be rather different. The natural dynamics to study for an Ising model is the relaxation process in which spins flip independently but remain in equilibrium with a heat bath at temperature T . Following Glauber,²¹ we take the probability for the spin S_i to flip to be given by

$$w(S_i) = S_i \left(1 - \frac{1}{2} (1 - S_i) \tanh \beta h_i \right), \quad (5.8)$$

where the unit of time, or the rate at which spin flips are attempted, is set equal to unity, and the change in energy upon flipping the spin S_i is given as $h_i S_i$, with h_i a molecular field. The form (5.8) satisfies detailed balance, and thus assures that the correct equilibrium distribution of microstates is attained. Suzuki and Kubo²² in a classic paper, have developed a mean-field theory of relaxation processes governed by (5.8). Their theory has recently been extended to treat the random molecular fields found in the infinite-ranged Ising spin-glass with $\bar{J} = 0$ by Kinzel and Fischer.²³ To shorten the derivations, we shall follow these two papers closely, although our treatment differs from that of Kinzel and Fischer in an essential step.

Averaging a master equation based on (5.8), Suzuki and Kubo find that the time dependence of the order parameter in the usual ferromagnetic case is governed by

$$\frac{d}{dt} \langle S_i(t) \rangle = \langle S_i(t) \rangle + \frac{1}{2} \tanh \beta h_i(t). \quad (5.9)$$

A mean-field solution to (5.9) is obtained²² by assuming that unique values of $\langle S_i(t) \rangle$ and $h_i(t)$ exist and are proportional

$$\lambda g(t) = \lambda S(t), \quad (5.10)$$

Then, expanding the tanh in powers of its argument, one obtains

$$\frac{d}{dt} g(t) = -(1 + \lambda g(t)) - (\lambda^2/2) g^2(t), \quad (5.11)$$

valid for temperatures close to or above T_c . Integration of (5.11) is straightforward. For $T = T_c$ the result is

$$g(t, T = T_c) = \frac{(1 + t)^{-1/2}}{[1 + (1 + t)^{-1/2} \exp(-2 \exp(-1/2))]} \quad (5.12)$$

decaying exponentially to zero as $e^{-(1/2)t}$. From (5.10) and (5.12), we identify $\lambda = T_c/T$. As $\lambda \rightarrow 1$, the solution exhibits critical slowing down, changing over to a power law decay.

$$g(t, T_c) = (1 + t)^{-1/2} \quad (5.13)$$

with the critical exponent $-1/2$. Below T_c , exponential relaxation again occurs, this time to a nonzero equilibrium limit, $g_c(T)$:

$$g(t, T < T_c) = \frac{g_c(T)}{[1 + (1 - g_c(T)) \exp(-\lambda g_c(T) t)]}. \quad (5.14)$$

For the spin correlations of interest in the present case, Kiazee and Fischer¹⁷ have used similar arguments to obtain the kinetic equation:

$$\frac{d}{dt} \langle S_i S_j(t) \rangle = \langle S_i S_j(t) \rangle + \langle S_i \rangle \text{tanh} \langle S_j(t) \rangle, \quad (5.15)$$

where $\langle S_i \rangle$ here denotes $\langle S_i(t=0) \rangle$, and

$$\begin{aligned} \frac{d}{dt} \langle S_i(t) S_j(t) \rangle &= 2 \langle S_i(t) S_j(t) \rangle + \langle S_i(t) \rangle \text{tanh} \langle S_j(t) \rangle \\ &\quad + \langle S_j(t) \rangle \text{tanh} \langle S_i(t) \rangle, \end{aligned} \quad (5.16)$$

to the steady state, (5.16) determines the equilibrium correlations,

$$\langle S_i S_j \rangle_{eq} = \langle S_i \rangle \text{tanh} \langle S_j \rangle_{eq}. \quad (5.17)$$

In a spin-glass, it will not be valid to treat $\langle S_i S_j(t) \rangle$ or $\langle S_j(t) \rangle$ as spatially uniform, since in fact S_j will fluctuate about zero. Also, the expression for $\langle S_j \rangle$ commonly employed when treating static properties in the mean-field approximation, $\langle S_j \rangle = \langle \sum_{\mu} J_{\mu j} S_{\mu} \rangle$, gives incorrect results when one attempts to calculate susceptibility, as Braks and Thomas¹⁸ have pointed out. The remedy was originally noted by Onsager.¹⁹ One must remove from $\langle S_j \rangle$ the field of the extra moment induced on neighboring sites by the presence of the moment $\langle S_j \rangle$. This is

$$\langle S_j \rangle = \chi_{jj}^{-1} \langle S_j \rangle + \chi_{jk} \langle S_k \rangle, \quad (5.18)$$

where we have used a simplified expression for χ_{ij}^{-1} , valid only above the ordering temperature,

Subtracting the effect of (5.18) from $\langle S_j \rangle$ in (5.17) leaves

$$\langle S_j \rangle = \sum_k (J_{jk} \langle S_k \rangle - \chi_{jk} \langle S_j \rangle). \quad (5.19)$$

This expression for $\langle S_j \rangle$ was rediscovered by TAP, who derive it by several independent arguments. They found that without the second term it is impossible to calculate even static properties of a spin-glass correctly in the infinite-ranged limit.²⁰

Substituting (5.19) into the kinetic equation (5.15) and keeping only the linear term in the expansion of tanh $\langle S_j \rangle$ leads to

$$\left(1 + \frac{d}{dt} + \sum_k J_{jk}^2\right) \langle S_i S_j(t) \rangle = \sum_k J_{jk} \langle S_i \rangle \langle S_k(t) \rangle, \quad (5.20)$$

So that

$$\sum_k J_{jk}^2 = J^2 + \left\langle \left(\frac{1}{N}\right) \right\rangle \quad (5.21)$$

by (2.2b), the left-hand side of (5.20) is independent of i . Equation (5.21) can now be solved by expanding the solution in terms of the eigenvectors of the random matrix whose components are J_{jk} . If

$$1 + \sum_k J_{jk}^2 = \lambda^2 + \langle q_j^2 \rangle, \quad (5.22)$$

the time decay of correlations can be expressed in terms of the independent relaxation frequencies λ .

Thus, we expand

$$\langle S_i S_j(t) \rangle = N^{-1} \sum_{\lambda} a_{\lambda}(t) \langle S_i^{(1+\lambda)} S_j^{(1-\lambda)} \rangle, \quad (5.23)$$

then

$$a_{\lambda}(t) = a_{\lambda}(0) \exp[-(1 + \lambda^2 J^2 + \langle q_j^2 \rangle)t]. \quad (5.24)$$

The $a_{\lambda}(0)$ are readily calculated by expanding the equilibrium correlations as in (5.23) and substituting into (5.17). The result is

$$a_{\lambda}(0) = (1 + 4 J^2 J^2 + \langle q_j^2 \rangle)^{-1/2}. \quad (5.25)$$

Note that if the J_{jk} were not random but constant, as in the infinite-ranged ferromagnet, the largest eigenvalue of the matrix would be J_{jj} , and all other eigenvalues would be zero. Thus, only one mode contributes to the decay of correlations in a ferromagnet in the near-Mott limit. In contrast, there is a continuous spectrum of λ for the spin-glass, and its density takes the simple form¹⁹

$$N^{-1} \sum_{\lambda} = (2\pi J^2 J^2)^{-1} \int_{-J}^{+J} d\lambda (2 J^2 - \lambda^2)^{1/2}. \quad (5.26)$$

introducing $x = \lambda - 2\beta\bar{J}$ and combining (5.25)–(5.26), we obtain the linearized result, valid for $T > T_g$:

$$\langle S_i S_j(t) \rangle = \exp[-(1 - 3\bar{J})^2 t] \times \int_0^1 dx \frac{(2+x)(1-x)^{1/2} e^{-x/2} + \pi \bar{J}^{1/2} e^{-x/2}}{(1-3\bar{J})^2 + 23\bar{J}(1-x)^2}. \quad (5.27)$$

In the high temperature limit, the integral in (5.26) can be evaluated by neglecting terms of order \bar{J} in the denominator, with the result

$$\langle S_i S_j(t) \rangle = e^{-(1-3\bar{J})^2 t} e^{-(2\bar{J})^2 t} (23\bar{J})^2 t \\ = \exp[-(1-3\bar{J})^2 + 2\pi^{1/2}\bar{J} t^{1/2}]. \quad (5.28)$$

This result, like the ferromagnetic solution (5.12), exhibits critical slowing down as T decreases to $T_g = 1/T_c$. Unlike the ferromagnetic system, the spin-glass has a correlation decay rate proportional to $|(T - T_g)/T|$, so the effects of the critical slowing-down should be observable over a wider range of temperatures in the spin-glass than in the ferromagnet.

In studies of dynamical critical phenomena,²² it is conventional to interpret the characteristic time τ for order parameter relaxation as the ratio

$$\tau = \chi^{(2)}(T - T_g)/T(T - T_g), \quad (5.29)$$

of the order parameter susceptibility there, $\chi^{(2)}$ to a friction coefficient Γ . In a mean-field theory, one expects that fluctuations in the order parameter will cause χ to diverge as $(T - T_g)^{-\Gamma}$. For spin glasses, Fitch and Harris²³ have confirmed that this value of the susceptibility exponent is reached at sufficiently high dimensionality, by analysis of series expansions of $\chi^{(2)}$. This implies that $\Gamma = 0$ as $\lambda \rightarrow T_g$ for spin-glasses, which in most mean-field theories, Γ remains finite at T_g . This unusual behavior is consistent, however, with the general picture of the spin-glass transition temperature T_g as the point at which blocking effects (TAP) or "frustration" suddenly set in.

Monte Carlo calculations of $\langle S_i S_j(t) \rangle$, using the Glauber dynamics (5.8) were carried out at several temperatures, both above and below T_g . The results above T_g are compared with the predictions of the linearized theory (5.27) in Figs. 13(a)–13(c). The integral in (5.27) was performed numerically to obtain the plotted curves. Each sample studied in the Monte Carlo simulations had 850 spins, and two samples were considered in each of Figs. 13(a)–13(c). Before beginning the collection of data on $\langle S_i S_j(t) \rangle$, 100–200 time steps per spin were taken to allow the samples to come to equilibrium at the desired temperature. In each of the three cases, the observed decay of correlations was slower than as predicted by the linearized theory,

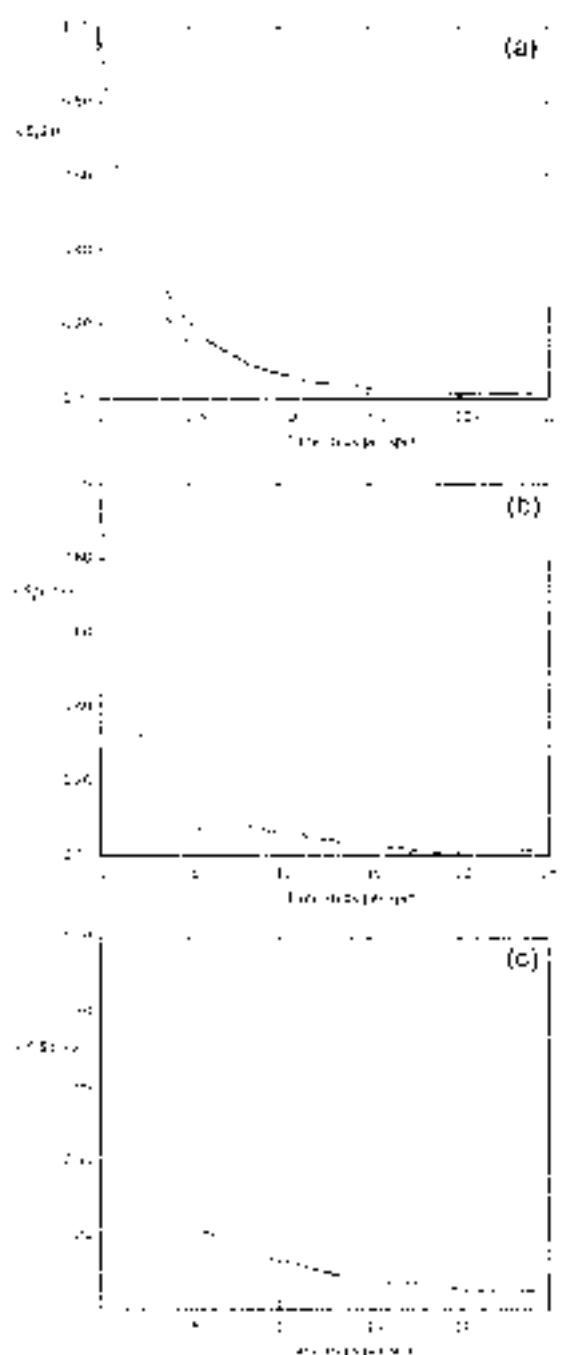


FIG. 13. (dashed lines) indicate the decay of spin correlations predicted by the linearized molecular-field theory in (5.27). The closely spaced data are Monte Carlo data for two samples with 850 spins. Cases shown are (a) $T = 2.07T_g$, (b) $T = 1.57T_g$, and (c) $T = 1.25T_g$.

but the error seen at the highest temperature, $T = 2.07T_g$ [Fig. 13(a)] is fairly small. Agreement is still fair at $T = 1.57T_g$ [Fig. 13(b)], but begins to become poor at $T = 1.25T_g$ [Fig. 13(c)].

Evaluating (5.27) at T_g , where $\lambda = 1$, gives²²

$\langle S_i S_j(t) \rangle \sim t^{-1/2}$, the same asymptotic dependence as seen in the single-field result (5.13). The similarity is probably coincidental, since (5.27) leaves out the nonlinear restoring term in (5.11) which is the source of the $t^{-1/2}$ limiting behavior in (5.12). It is difficult to add such nonlinear terms to the treatment leading up to (5.67) since these will mix the modes which have been treated as independent. Ma and Rudnick¹ have recently studied spin-glass dynamics in a nonlinear mean-field approximation. Their model, a scalar Landau-Ginzburg-Wilson Euclidian with a random molecular field, may be applicable to the present simulations. They find $\langle S_i S_j(t) \rangle \sim t^{-1/2}$ for long times, not only at T_g but also at all lower temperatures. However, their calculation gives $\tau = 17 - 2.5T$ above T_g , in contrast to (5.20).

Our Monte Carlo results agree below T_g are consistent with Ma and Rudnick's prediction. At temperatures below T_g , $\langle S_i S_j(t) \rangle$ does not decay exponentially as it would in a ferromagnet [see (5.14)]. Data for $T = T_g$, $0.8T_g$, and $0.6T_g$ are shown in Fig. 14. A plot of $\langle S_i S_j(t) \rangle^{-1} - 1$ against t , using the $T = T_g$ data of Fig. 14, have a straight line for the first 25 time steps per spin. At longer times, the statistical fluctuations due to the finite number of spins swamped any further decrease in $\langle S_i S_j(t) \rangle$. Thus, the data taken at T_g can be described as $\langle S_i S_j(t) \rangle \sim (1 - \alpha t)^{-1/2}$ where α is a phenomenological constant which turns out to be not too different from the τ obtained in (5.13).

Below T_g , an extension of (5.13),

$$\langle S_i S_j(t) \rangle \sim (1 - q_0)(1 - \alpha t)^{-1/2} + q_{\infty} \quad (5.30)$$

gives an excellent fit to the data. The heavy em-

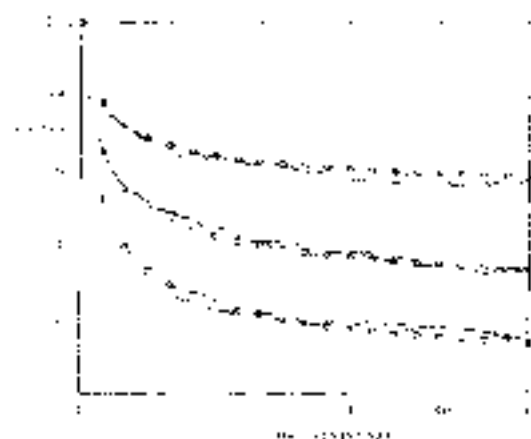


FIG. 14. Monte Carlo data on the time dependence of spin correlations are shown as in Fig. 13 for three temperatures: (top) $T = T_g$, (middle) $T = 0.8T_g$, and (bottom) $T = 0.6T_g$. Four samples of 500 sites each were used at each temperature. The curves are fitted by phenomenological equation (5.30), containing a $t^{-1/2}$ decay.

dash in Fig. 14 indicates fits of the form (5.30) using $q_0 = 0, 0.22$, and 0.49 for $T = T_g, 0.8T_g$, and $0.6T_g$, respectively, and values of α between 1.0 and 2.85. These values of q_0 were chosen to agree with the long-time-averaged values of the EA order parameter expected from theory [see (2.10)] and as observed and shown in Fig. 11.

No choice of parameters in an expression of the form (5.14) gives an adequate fit to the data $T = 0.8$ or $0.6T_g$. If the known long-time limiting values of $q(T)$ are used and the initial slope is taken as a free parameter, (5.14) reaches its limiting value too rapidly. If we force agreement with the data for 25–50 time steps per spin, (5.14) gives too small an initial rate of decay.

Binder² has described a similar slow decay of the EA order parameter in Monte Carlo studies in two- and three-dimensional Ising models with random exchange interactions governed by a Gaussian distribution, but he did not assign a functional form to the decay. Since the EA order parameter does not relax rapidly to its equilibrium value at temperatures $< T_g$ as the magnetization, governed by (5.14), would for a ferromagnet, Binder has questioned whether some other order parameter might be constructed with more conventional behavior.

We do not think this likely. In the infinite-ranged spin-glasses, we have demonstrated that q is the order parameter which uniquely characterizes the spin-glass phase. The Monte Carlo simulations show that even in this mean-field limit, $q(t)$ exhibits nonexponential relaxation at all $T < T_g$. The linearized analysis of dynamics supports that the existence of a continuous spectrum of relaxation rates extending to zero is sufficient to introduce power law decay¹⁰ of correlations. Thus, the unusual time dependence of the EA order parameter seems to be a signature of the spin-glass state.

VIII. CONCLUSIONS

In this paper we have investigated the properties of spin-glass models with infinite-ranged random exchange interactions, both analytically and by means of computer simulation experiments. The discussion has been presented mainly, but not exclusively, in terms of Ising spins. Consideration has been given to four theoretical approaches: (i) a replication procedure^{1,2} in which the random system is mapped at the outset into a limiting case of a fictitious pure system with extra spin labels and higher-order interactions, (ii) high-temperature series expansion,⁴ (iii) a mean-field theory allowing for a different mean field on each site and deferring all averaging to the end of the calculation,⁶ and (iv) a MFT approximation.^{11–13} Only

the first three of these approaches claim any degree of rigor, the fourth being heuristic.

In this paper we give a detailed derivation of the first approach, and briefly review the others. The second and third theories are discussed at length in Ref. 8. Computer experiments presented are of three kinds: (a) investigation of the structure of the low-energy states of the system, (b) Monte Carlo simulation of the equilibrium thermodynamics, and (c) Monte Carlo simulation of dynamics.

The replica procedure has been solved subject only to making an interchange of limits (the thermodynamic limit, $N \rightarrow \infty$, and a limit on the number of replicas, $n \rightarrow 0$). The procedure predicts a phase diagram with two types of magnetically ordered phases, ferromagnet and spin-glass. The spin-glass to paramagnet transition manifests itself by cusps in the zero-field susceptibility (which is rounded in the presence of an external field) and in the specific heat. At all but the lowest temperatures, the predicted thermodynamic functions are physical but at low temperatures the procedure yields a finite negative entropy.

The high-temperature series expansion can be summed exactly in the thermodynamic limit and predicts phase transitions from paramagnet to ordered phases at the same temperatures as found by the replica method. In the paramagnetic phase, analysis of the high-temperature series in zero magnetic field confirms all the corresponding equilibrium thermodynamic predictions of the replica procedure. The third theoretical approach (TAP) has been studied in detail only for a particular case of the general model which can be treated by the replica procedure, namely the case with nearest exchange and external field equal to zero. Approximate solutions within this approach, believed reliable in the thermodynamic limit for temperatures above and close to the spin-glass transition temperature T_g , are in complete accord with the replica results above T_g and agree to the leading order in $(T_g - T)$ immediately below the transition. At low temperatures, however, the TAP procedure when coupled with an ansatz for the solution (based upon limited computer simulations and physical intuition) leads to results somewhat different from those of the replica method. In particular, it does not exhibit the unphysical negative entropy.

Monte Carlo simulations were performed on samples of up to 800 spins with infinite-ranged interactions to test the predictions of the various theories and to provide quasistatistical information about the low-temperature phase of a spin-glass. The ground-state energy predicted by the replica method lies slightly lower than the Monte

Carlo results, the difference exceeding the probable error in the simulations. The discrepancy between the predicted internal energy and Monte Carlo observations becomes insignificant at temperatures greater than $0.5T_g$, and at all temperatures when the mean value of the exchange interactions was sufficiently great for the system to remain ferromagnetic at the lowest temperatures.

The entropy was determined by integrating the internal energy found by simulation. To within the accuracy of simulations $\lim_{T \rightarrow 0} S(T) = 0$. The absolute difference between the replica theory prediction for $S(T)$ and observation becomes small for $T > 0.5T_g$.

The TAP expression for the limiting behavior of $S(T)$ at low temperatures gives good agreement with the Monte Carlo results. Simulations of the specific heat and the susceptibility are also in good agreement with the TAP ansatz.

An attempt was made to quantify the degeneracy of the spin-glass ground state by counting the number of distinct local energy minima. The minima were found to occur in groups, which may be thought of as large "valleys" in phase space. Both the number of minima and the number of valleys appears to increase with N , the number of spins, as some small power of N . They therefore do not give rise to a finite entropy at $T = 0$.

The distribution of exchange fields in the spin-glass ground state was obtained in the course of the simulations and compared with the distribution assumed in the mean-random-field approximation. The two distributions prove to be very different.

Linearized random kinetic equations for the decay of spin correlations above T_g are derived and solved. They give good agreement with Monte Carlo studies of spin relaxation for $T > 1.5T_g$. At and below T_g the decay of $\langle S_i S_j(t) \rangle$ to its long time limit, the Edwards-Anderson order parameter q is slower than exponential. It can be accurately described by a $t^{-1/2}$ law.

ACKNOWLEDGMENTS

One of us (D.S.) would like to thank the Directors of the IBM T.J. Watson Research Center and the Institut Louis-Langevin for extending to him the hospitality of their organizations, and particularly to Dr. S. von Molnár for arranging his visit to IBM, which led to the authors' collaboration. We would like to thank D. J. Thouless, P. W. Anderson, and R. G. Palmer for stimulating discussions of their work prior to its publication. Conversations with T. C. Lubensky, E. Pytte, and J. Rudnick, and preprints received from G. Toulouk, A. P. Young, and K. Binder are also gratefully acknowledged.

APPENDIX A

The matrix A of Eq. (2.13) is conveniently expressed in the basis $\{e^i\}$, the general member of which we shall denote by e^i , where i runs from 1 to $n(n+1)$. The xx matrix element of A is $e^i \cdot g(\{s\}) / \partial x^i \partial x^j$ where $-N g(\{s\})$ is the exponent of the exponential integrand of (2.10). The derivatives are evaluated with all $e^i = v^i$ set equal to x_{av} , y_{av} and expressed in terms of ω_x, q , using (2.12). Thus,

$$\frac{\partial^2 g}{\partial x^i \partial x^j} = -\delta_{ij} \left(1 - \frac{\partial x}{\partial t}\right) \\ = -(1 - \delta_{ij}) \left(\frac{\partial x}{\partial t}\right) q_{\text{av}} \left(\frac{\partial x}{\partial t}\right) \omega_x^2, \quad (\text{A1})$$

$$\frac{\partial^2 g}{\partial y^i \partial y^j \partial x^k} = \delta_{ijk} \omega_x \left[1 - \left(\frac{\partial x}{\partial t}\right)^2\right] - (1 - \delta_{ij}) \omega_x \omega_y \\ \times \left(\frac{\partial x}{\partial t}\right)^2 q_{\text{av}} (t_{\text{av}} + t_{\text{av}} - \delta_{ij} t_{\text{av}} + \delta_{ij} t_{\text{av}}) \\ = (1 - \delta_{ij}) \delta_{ik} (1 - \delta_{jk}) (1 - \delta_{ij}) \\ \times \left(\frac{\partial x}{\partial t}\right)^2 \omega_x^2 \omega_y^2 q_{\text{av}} + \left(\frac{\partial x}{\partial t}\right)^2 q_{\text{av}}^2, \quad (\text{A2})$$

$$\frac{\partial^2 g}{\partial y^i \partial x^j \partial x^k} \\ = -\left(\frac{\partial x}{\partial t}\right)^2 \left(\frac{\partial x}{\partial t}\right) [(\delta_{ik} - \delta_{jk}) \omega_x \\ = (1 - \delta_{ik}) - \delta_{jk} + \delta_{ik} \delta_{jk} q_{\text{av}}], \quad (\text{A3})$$

where

$$\langle S^i S^j S^k \rangle_{\text{av}} = \frac{k_B (2\pi)^{-1/2} \exp(-\frac{1}{2} \Delta^2) \tanh^2 \Xi \cosh^2 \Xi}{\int dz (2\pi)^{-1/2} \exp(-\frac{1}{2} z^2) \cosh^2 \Xi}, \quad (\text{A4})$$

and

$$\langle S^i S^j S^k S^l \rangle_{\text{av}} = \frac{\int \frac{dz}{(2\pi)^{1/2}} \exp(-\frac{1}{2} z^2) \tanh^2 \Xi \cosh^4 \Xi}{\int \frac{dz}{(2\pi)^{1/2}} \exp(-\frac{1}{2} z^2) \cosh^2 \Xi} \quad (\text{A5})$$

APPENDIX B

In this Appendix, we demonstrate explicitly that

$$\alpha = \beta \langle S_1^2 \rangle_0, \quad (\text{B1})$$

$$q = \langle (S_1^i)^2 \rangle_0, \quad (\text{B2})$$

where α and q are the averages introduced in Sec. II, and defined by

$$\alpha = \lim_{n \rightarrow 0} \langle S_1^2 \rangle_n \text{Tr}_n \exp(-\beta H_n^{\text{eff}}), \quad (\text{B3})$$

$$q = \lim_{n \rightarrow 0} \langle S_1^i S_1^i \rangle_n \text{Tr}_n \exp(-\beta H_n^{\text{eff}}) = \alpha \ell^2, \quad (\text{B4})$$

where Tr_n denotes an average in the n -replica

system characterized by the effective Hamiltonian defined by

$$\exp(-\beta H_n^{\text{eff}}) = \int \prod_i d\phi_i \rho(\phi_i) \exp\left(-\beta \sum_i \phi_i^2\right).$$

This result is true for any distribution $\rho(\phi_i)$ and not restricted to the infinite-ranged models discussed in this paper.

The thermal average of the spin at any site i is given by

$$\langle S_i \rangle = \text{Tr} S_i \exp(-\beta H) / \text{Tr} \exp(-\beta H). \quad (\text{B5})$$

Thus,

$$\sum_i \langle S_i \rangle = -\frac{1}{\partial \phi} \lim_{\phi \rightarrow 0} \text{Tr} \exp\left(-\beta H - \phi \sum_i S_i\right) \Big|_{\phi=0} \\ = -\frac{1}{\partial \phi} \lim_{\phi \rightarrow 0} \phi^{-1} \\ \times \left[\text{Tr}_n \cosh\left(-\beta \sum_i \phi^2 - \phi \sum_i S_i\right) + 1 \right]_{\phi=0}. \quad (\text{B6})$$

Averaging over S_i , we therefore find

$$\langle S_i \rangle_0 = (1/\partial \phi) \lim_{\phi \rightarrow 0} \phi^{-1} \frac{\partial}{\partial \phi} \\ \times \left[\text{Tr}_n \exp\left(-\beta \sum_i \phi^2 - \beta \phi \sum_{i,j} S_i^2 S_j^2\right) + 1 \right]_{\phi=0}, \quad (\text{B7})$$

where the effective Hamiltonian was given in (2.6):

$$H_n^{\text{eff}} = - \sum_{i,j} \left(\sum_{\alpha} S_i^{\alpha} S_j^{\alpha} \phi_{\alpha} + \sum_{\alpha\beta} S_i^{\alpha} S_j^{\alpha} S_i^{\beta} S_j^{\beta} \phi_{\alpha\beta}^2 \right) \\ = H \sum_i S_i^2. \quad (\text{B8})$$

Thus,

$$\langle S_i \rangle_0 = \lim_{n \rightarrow 0} \text{Tr}_n (n N^{1/n} \sum_{i,j} S_i^2 \exp(-\beta H_n^{\text{eff}})) \\ = \lim_{n \rightarrow 0} \langle S_1^2 \rangle_n \text{Tr}_n \exp(-\beta H_n^{\text{eff}}) = \alpha. \quad (\text{B9})$$

Similarly,

$$\sum_i \langle S_i^i \rangle^2 = 4^{-1} \frac{\partial}{\partial \phi_{ii}} \ln \text{Tr}_{n,i} \exp\left(-\beta (\phi_{ii} + \alpha^2) \sum_i S_i^i S_i^i\right) \\ = 4^{-1} \alpha \ell^2 \sum_i \langle S_i^i S_i^i \rangle, \quad (\text{B10})$$

where i, i' label distinct replicas,

$$\sum_i (S_i^x)^2 = \beta^{-1} \frac{\partial}{\partial h_{xy}} \lim_{n \rightarrow 0} n^{-1} \text{Tr}_{\mathcal{H}_n} \times \exp \left(-\beta \sum_i (v_i^{xx} + v_i^{yy}) + \beta h_{xy} \sum_{i,j} S_i^x S_j^y \right), \quad (10)$$

Averaging over J_{ij} and explicitly performing the h_{xy} differentiation we obtain

$$\begin{aligned} \langle S_i^x \rangle^2 &= \lim_{n \rightarrow 0} \text{Tr}_{\mathcal{H}_n} (h_{xy})^{-1} \sum_{i,j} S_i^{xx} S_j^{yy} \exp(-\beta S_i^{xx} S_j^{yy}) \\ &= \lim_{n \rightarrow 0} \langle S_i^x S_j^y \rangle_{\mathcal{H}_n} \text{Tr}_{\mathcal{H}_n} \exp(-\beta S_i^{xx} S_j^{yy}) \quad (\alpha \neq \beta) \\ &= \lim_{n \rightarrow 0} n^{-1} \text{Tr}_{\mathcal{H}_n} \exp(-\beta S_i^{xx} S_j^{yy}) \\ &= \lim_{n \rightarrow 0} q_{\alpha} \text{Tr}_{\mathcal{H}_n} \exp(-\beta S_i^{xx} S_j^{yy}) = q, \end{aligned} \quad (11)$$

* Permanent address.

† Present address.

¹For a review of earlier related work, see V. Cannella and J. A. Mydosh, *Adv. Conf. Proc.*, **10**, 651 (1974); J. A. Mydosh, *Amorphous Magnetism II*, edited by R. A. Levy and B. Eisenstein (Plenum, New York, 1977), p. 73.

²For reviews of theoretical work, see R. H. Fisher, *Physica Scripta* **25**, 410 (1975); R. Fisher, *Fortschritte der Physik (Advances in Solid State Physics)*, edited by J. Treusch (Vieweg, Braunschweig, 1977), p. 15; J. Sherrington, *Adv. Conf. Proc.*, **20**, 225 (1976), and report for Aspen's Conference on Glasses and Spin Glasses, March, 1977 (unpublished).

³S. F. Edwards and D. W. Anderson, *J. Phys. F*, **2**, 961 (1972). We refer to this paper as EA.

⁴K. H. Fischer, *Phys. Rev. Lett.*, **32**, 1158 (1974).

⁵J. Sherrington and S. Kirkpatrick, *Phys. Rev. Lett.*, **37**, 1792 (1976).

⁶D. Sherrington and D. W. Southwell, *J. Phys. F*, **2**, 149 (1972).

⁷See, e.g., E. E. Snider, *Phase Transitions and Critical Phenomena* (Acad. C. P., New York, 1975), p. 31.

⁸S. F. Edwards, D. W. Anderson, and R. G. Palmer, *Philos. Mag.*, **36**, 969 (1977). We refer to this paper as EAP.

⁹M. Kau, *Trondheim Theoretical Physics Seminar*, Nordby Publ. No. 296, 1968 (unpublished); and T. F. Lin, *J. Math. Phys.*, **11**, 1595 (1970).

¹⁰S. F. Edwards, *Proceedings of the Third International Conference on Amorphous Materials, 1975*, edited by R. W. Douglas and B. Ellis (Wiley, New York, 1976), p. 273; *Polymers Networks*, edited by A. J. Challa and S. Newman (Plenum, New York, 1977), p. 93.

¹¹G. Grestman, Ph.D. thesis (Harvard University, 1974) (unpublished); G. Grestman and A. H. Jahn, *Phys. Rev. B*, **12**, 1329 (1975).

¹²V. L. Kaluzh, *Phys. Rev. B*, **11**, 338 (1975).

¹³A. B. Harris, T. C. Lubensky, and J.-H. Chen, *Phys. Rev. Lett.*, **36**, 415 (1976); J.-H. Chen and T. C. Lubensky, *Phys. Rev. B*, **16**, 2405 (1977) (in press). Also R. G. Priest and T. C. Lubensky, *Adv. Phys.*, **21**, 4159 (1976) have used the reptation method as the basis for a renormalization group calculation for a spin-glass in 6+ε dimensions. Their free energy differs from (2.16), but is also a maximum, not a minimum, at the physical solution.

¹⁴J. M. Kosterlitz, R. J. Thouless, and R. C. Jones, *Phys. Rev. Lett.*, **36**, 1217 (1976).

¹⁵Diagrams with more complex topology are of order $N^{1/2}$ or less. Diagrams with mixed single and double bonds all fall into this category.

¹⁶S. Kirkpatrick and C. M. Varma, *Solid State Commun.*, to be published.

¹⁷R. L. Lawler, *Combinatorial Optimization* (McLaren-Hart and Winston, New York, 1976).

¹⁸S. Kirkpatrick, *Phys. Rev. B*, **16**, 4930 (1977).

¹⁹J. Vanhulst and G. Toulouse, *J. Phys. C*, **10**, 1307 (1977).

²⁰M. D. Gryn and S. M. Yohari, *Solid State Commun.*, **24**, 167 (1977).

²¹W. Marshall, *Phys. Rev.*, **71**, 1011 (1954).

²²M. W. Klein and D. Brans, *Phys. Rev.*, **132**, 124 (1963).

²³M. W. Klein, *Phys. Rev. B*, **14**, 5008 (1976).

²⁴R. J. Glauber, *J. Math. Phys.*, **4**, 291 (1963).

²⁵M. Suzuki and R. Kubo, *J. Phys. Soc. Jpn.*, **24**, 51 (1966).

²⁶W. Kinzel and K. H. Fischer, *Solid State Commun.*, **23**, 1071 (1977).

²⁷R. Israel and R. Thoms, *Phys. Rev. B*, **3**, 317 (1971).

²⁸W. Kinzel and K. H. Fischer (see note added in proof to Ref.

²⁷) have observed that the term $(\vec{p} \cdot \vec{J})^2$ on the left-hand side of the kinetic equation (5.23) is the manifestation of their formal renormalization in the form of $\gamma_{\vec{p}}$. They were guided to this observation by the appearance of such a $(\vec{p} \cdot \vec{J})^2$ corrective term in the spherical model calculation of Ref. 14. Similarly, R. Brout and H. Frenkel (Ref. 27) note that the spherical model differs from the conventional mean-field theory by adding just those terms necessary to satisfy the fluctuation-dissipation theorem. The physical content of this otherwise mysterious correction is evident from the discussion accompanying (5.24) and (5.19).

²⁹S. L. Madsen, *Random Matrices and the Statistical Theory of Energy Levels* (Academic, New York, 1967), p. 243; S. F. Edwards and R. C. Jones, *J. Phys. A*, **9**, 1593 (1976).

³⁰R. Hönlberg and B. L. Holgerin, *Rev. Mod. Phys.*, **48**, 475 (1977).

³¹R. Fisch and A. J. Harris, *Phys. Rev. Lett.*, **38**, 755 (1977).

³²G. Toulouse, *Commun. Phys.*, **2**, 115 (1977).

³³S. F. M. and J. Ruckelshaus, *Phys. Rev. Lett.*, **40**, 683 (1978).